Motion Fidelity Requirements for Helicopter-Ship Operations in Maritime Rotorcraft Flight Simulators

Wajih A. Memon,[*] Ieuan Owen,[†] and Mark D. White[‡]
University of Liverpool, Liverpool, England L69 3GH, United Kingdom

The research presented in this paper is part of a longer-term project to develop overall fidelity requirements for simulated helicopter shipboard operations to inform and support First of Class Flight Trials. The paper reports the results of motion cueing assessment and optimisation research, conducted in a six-degree-of-freedom motion flight simulator, to develop simulator motion drive laws capable of providing high fidelity motion cueing for simulated shipboard operations. To do this, a novel objective technique, Vestibular Motion Perception Error (VMPE), has been developed. The technique was utilised to optimise the motion cues for simulated helicopter landings on a naval single-spot destroyer at different wind and sea-state conditions. New simulator motion tuning sets were derived offline and then tested experimentally to compare the objective VMPE predictions with subjective assessments from a test pilot. Results show the influence of different motion cues, airwake conditions and ship motion states on the pilot's overall perception of self-motion, control strategy, task performance and workload. It was found that high-fidelity motion cueing becomes more desirable for the pilot at higher wind conditions and sea states, for which an 'Optimised' motion setting was obtained using the new technique. Moreover, the use of an 'Optimised' motion setting generated by the VMPE methodology resulted in reduced pilot workload, leading to improved simulated maritime helicopter operational capability. The technique provides a rational methodology for motion tuning which could be applied in training and engineering simulators.

[*]Ph.D. Candidate, Flight Science & Technology Research Group, The University of Liverpool.
[†]Emeritus Professor of Mechanical Engineering, School of Engineering, The University of Liverpool.
[‡]Senior Lecturer, Flight Science & Technology Research Group, The University of Liverpool.

Nomenclature

a_x, a_y, a_z	=	aircraft linear body accelerations in x, y, z directions at c.g., m/s^2
a_{xs}, a_{ys}, a_{zs}	=	simulator linear body acceleration demands in x, y, z directions, m/s^2
F_{A_Per}, F_{S_Per}	=	perceived specific forces in aircraft and simulator at pilot vestibular centre, rad/s
F_{AA}	=	aircraft specific forces vector at aircraft's c.g., m/s^2
f_i-*per*	=	perceived specific forces at pilot vestibular centre (i=axis), m/s^2
F_{RC}	=	aircraft specific forces vector at the rotational centre of the simulator, m/s^2
F_{s_P}	=	simulator specific forces vector at pilot vestibular centre, m/s^2
F_{sp}-*x*	=	actual specific forces in x axis at pilot vestibular centre, m/s^2
F_{s_RC}	=	simulator specific forces vector at rotational centre of the simulator, m/s^2
f_x, f_y, f_z	=	aircraft specific forces in x, y, z, directions at c.g, m/s^2
f_{xs}, f_{ys}, f_{zs}	=	simulator specific forces in x, y, z, directions at rotational centre of the simulator, m/s^2
g_x, g_y, g_z	=	aircraft acceleration due to gravity, body reference frame, m/s^2
g_{xs}, g_{ys}, g_{zs}	=	simulator acceleration due to gravity, body reference frame, m/s^2
k	=	motion drive algorithm washout filter gain
k_{tilt}	=	motion drive algorithm washout filter gain for tilt channel
p, q, r	=	roll, pitch, yaw angular velocities of the aircraft, deg/s
R	=	position vector from aircraft centre of gravity to simulator rotational centre, m
$RMSE_{VMPE\_F}$	=	rmse of the perceived specific forces between aircraft and simulator, ft/s^2
$RMSE_{VMPE\_\omega}$	=	rmse of the perceived angular rate between aircraft and simulator, deg/s
r_p	=	position vector from aircraft centre of gravity to pilot vestibular centre, m
r_z	=	position vector from pilot vestibular centre to simulator rotational centre, m
u, v, w	=	aircraft linear velocities, m/s
u_s, v_s, w_s	=	simulator linear velocity demands, m/s
$VMPE_{RMSE\text{-}MTS\text{-}f}$	=	mean specific forces perception RMS error between aircraft and simulator, ft/s^2
$VMPE_{RMSE\text{-}MTS\text{-}\omega}$	=	mean angular velocity perception RMS error between aircraft and simulator, deg/s
X, Y, Z	=	linear aircraft displacements, ft
XA, XB, XC, XP	=	lateral, longitudinal, collective and pedal control inputs, %

ω_n = motion drive algorithm filter washout or break natural frequency, rad/s

ω_{tilt} = motion drive algorithm filter washout or break frequency for tilt channel, rad/s

ω_{AA} = aircraft angular velocity vector, rad/s

ω'_{AA} = aircraft angular acceleration vector, rad/s

ω_{A_Per}, ω_{S_Per} = perceived angular rates in aircraft and simulator, deg/s

ω_s = simulator angular velocity vector, rad/s

ω_i-*per* = perceived angular velocity (i=axis), rad/s

ω_{sp}-*y* = actual angular velocity (pitch rate) in y axis, rad/s

ω'_s = simulator angular acceleration vector, rad/s^2

ϕ, Θ, ψ = aircraft angular displacement, rad

ϕ_s, Θ_s, ψ_s = simulator angular displacement demands, rad

Subscripts

i = x, y, z axis

n = motion washout filter axis

Superscripts

m = number of dominant motion axis

N = length of the data vector

I. Introduction

NAVIES of various nations regularly perform helicopter launch and recovery operations to and from their ships. These operations are carried out in challenging conditions which are unique to the maritime environment. The combination of a confined ship deck landing space, together with irregular ship motion, sea spray and unsteady airflow over and around the ship's deck and superstructure, produce high risk operational demands on the helicopter, ship and crew. Together, these elements form the Helicopter Ship Dynamic Interface (HSDI) environment [1] (Fig. 1).

To determine the limitations of the safe operability of helicopters to/from ships, a safety envelope is constructed, normally through First of Class Flight Trials (FOCFTs), to determine Ship Helicopter Operating Limits (SHOLs) for every in-service combination of helicopter and ship. The SHOL details the safe conditions for launch and recovery operations [2]. FOCFTs are performed at sea and are inevitably very expensive and can typically take weeks to constr-

Fig. 1 HSDI environment

-uct a full SHOL envelope. Often the full range of wind and sea conditions (e.g., wind magnitudes and azimuths, sea states) may not be available, resulting in the development of a more conservative SHOL [3]. An example of a SHOL diagram for a helicopter operating to/from a frigate is shown in Fig. 2 (for winds from ±90° from ahead) [4]. The SHOL consists of radial and circumferential lines of wind azimuth and magnitude, respectively, representing the Wind Over Deck (WOD) condition (i.e., wind speed and direction relative to the ship). Winds coming from the port and starboard sides are denoted Red and Green winds, respectively. The SHOL limit is shown as a bold black line, and the area inside this boundary indicates the combinations of relative wind speed/direction for which it is deemed safe to land.

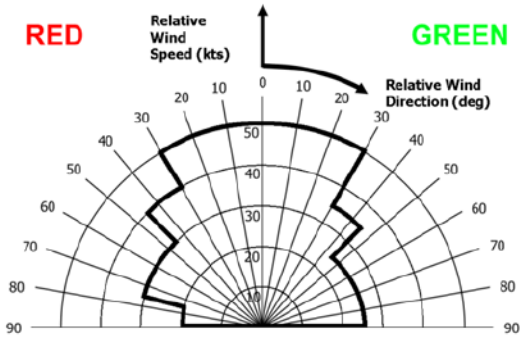

Fig. 2 Typical SHOL diagram [4]

Modelling and Simulation (M&S) tools are being developed and deployed in flight simulators to investigate these operational and meteorological risks, with the aim of making SHOL testing safer, quicker, and more cost-effective [5-8]. Whilst they are not trying to fully replace at-sea testing, the M&S tools are aimed at informing the key test points or "Hot Spots" of uncertainty to test at sea. The reliability of this support depends upon the identification of the fidelity requirements of the HSDI M&S elements integrated into the flight simulation environment, such as motion and visual cueing, the flight dynamics model, and the integration into the simulation of the unsteady airflow of the ship's airwake

[6].

Attempts have been made to assess the fidelity of research and maritime engineering rotorcraft simulators, e.g., the Joint Shipboard Helicopter Integration Process (JSHIP) project, which examined the viability of the use of flight simulators in defining SHOLs [6]. Moreover, helicopter-ship research undertaken at the University of Liverpool (UoL) Flight Science and Technology (FS&T) research group has examined the effect of motion, visual and airwake fidelity on overall simulation fidelity, pilot workload, task performance and subjective assessment [9-12]. FS&T has been at the forefront of academic research to develop a high-fidelity HSDI simulation environment since 2003 [3,4,9-15]. Research has also been undertaken in-house to quantify the overall fidelity of rotorcraft simulations [16,17], for its use in design, development, training and qualification.

Current simulator qualification standards, CS-FSTD(H) [18] and 14 CFR Part 60 [19] provide guidelines for the assessment of the component, or predictive fidelity, of civil flight simulators which define the acceptable match of data between aircraft and simulators for training purposes. The components include elements of the cueing environment, such as motion, visual and sound system, control loading together with the flight dynamics model, and includes subjective fidelity evaluations focused on specific areas. The guidelines provide qualification performance standards for objective evaluation based on tolerances, i.e., acceptable differences between simulation and flight. However, it is not clear whether meeting these standards will guarantee good overall perceptual simulation fidelity which may be defined as "*the simulator that induces the pilot to behave in a similar way as in the real aircraft*" [20,21]. Whilst an assessment of the perceptual fidelity of the simulator is undertaken by an evaluation pilot during qualification, objective metrics for this type of assessment have still to be defined [16,17]. Moreover, these standards do not currently contain fidelity requirements for motion tuning and airwakes for civil HSDI applications, and military standards do not currently exist. Whilst existing literature provides qualification methods, especially for the civil training simulators, these are not necessarily directly applicable to research simulators. A standardized guideline to quantify and qualify the overall fidelity of research and engineering simulators is, therefore, a challenge which is yet to be fully addressed [22].

The research presented in this paper is part of a project which aims to achieve the following objective: "To undertake a structured examination of the M&S elements of the HSDI simulation environment to develop a new robust simulation fidelity matrix to support at sea flight trials". The examination includes the analysis, evaluation, and improvement of the visual and motion cues, the airwake integration process, and vehicle modelling. Moreover, it aims

to develop a robust simulation fidelity matrix which will help to define the requirements for components of the HSDI simulation that are needed to inform the "real-world" SHOL trials with a reliable level of confidence. Figure 3 shows the HSDI M&S elements integrated into UoL's six-degree-of-freedom simulator for use in pilot-in-the-loop simulations.

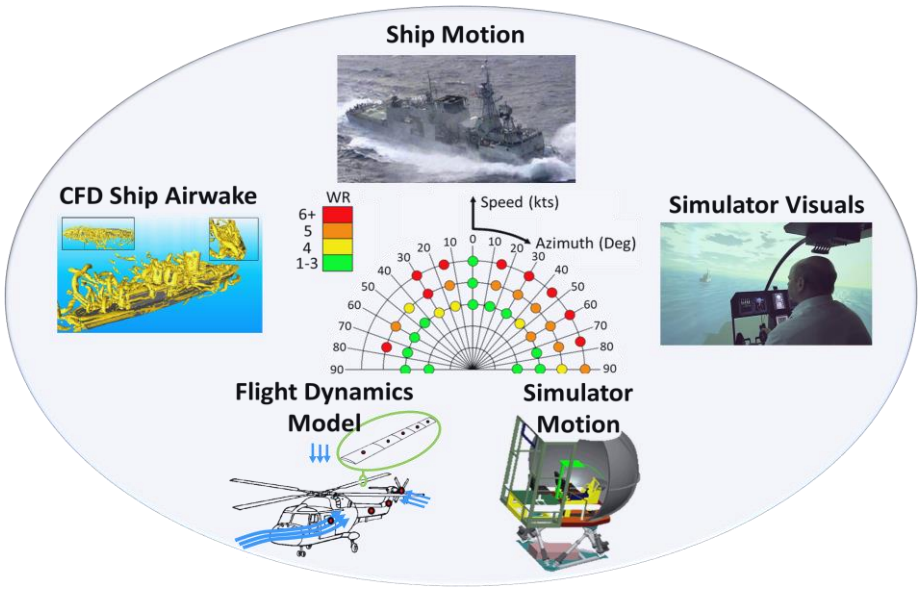

Fig. 3 HSDI modelling and simulation elements

Among the core elements of the HSDI M&S environment, motion cueing remains an important area of research due to a gap in existing knowledge regarding task-specific fidelity requirements, particularly in the highly dynamic HSDI environment. There is currently no robust tool available to efficiently and objectively tune the motion platform to allow the pilot to perceive "high-fidelity" motion cues in the HSDI environment despite significant research in land-based tasks [12,23-29], discussed in the next section. These studies have shown that motion cueing requirements can be task-specific which means that for each task, the simulator's motion must be tuned based on the dominant axis and the requirements of the task [23]. Therefore, it is difficult to obtain a single motion setting which can be universally used in different tasks to provide effective motion cues to the pilot. The factors which affect the pilot's motion perception are determined by the motion platform and configuration of the Motion Drive Algorithm (MDA) [30]. The focus of the research reported in this paper is the objective tuning of the MDA to optimise the vestibular motion cues for deck landing tasks performed in rotorcraft flight simulators.

II. Motion Cueing: Principles and Background

Motion cues in a flight simulator are perceived from visual information projected onto the human eye (i.e., visual motion cues, also known as vection), and from the simulator's motion platform movement detected by the vestibular system in the inner ear and proprioceptive/kinaesthetic cueing [31]. The vestibular system consists of two parts: the Semi-Circular Canals (SCC) and the Otoliths (Oto). The SCCs act as a damped angular accelerometer which senses the angular rates, whilst the Oto sense the specific forces obtained at the pilot Vestibular Centre (VC) [22,31,32].

Motion cues obtained from the simulator platform's physical movement should be in harmony with the motion cues obtained from the visual projection system. Poor synchronisation of the stimulation of optical flow cues and inertial motion cues can result in inaccurate visual and/or vestibular motion cues, leading to vague overall perception of self-motion, compromised subjective ratings and task performance from pilots during piloted simulation flight trials [33].

The motion platform demands of the flight simulator are produced by the MDA, which typically contain washout filters that tailor the simulator's motion response to provide a return to neutral capability. There are three main types of MDAs used in simulators: classical motion cueing washout algorithm, adaptive washout algorithm and optimal higher order motion drive algorithm. The most commonly used MDA is the Classical Washout Algorithm (CWA) proposed by Reid and Nahon [30], shown in Fig. 4. The CWA allows easy analysis of the filter settings and its response due to its linear filtering technique [34] and has been shown to achieve reasonably good results compared with the other two MDAs [35].

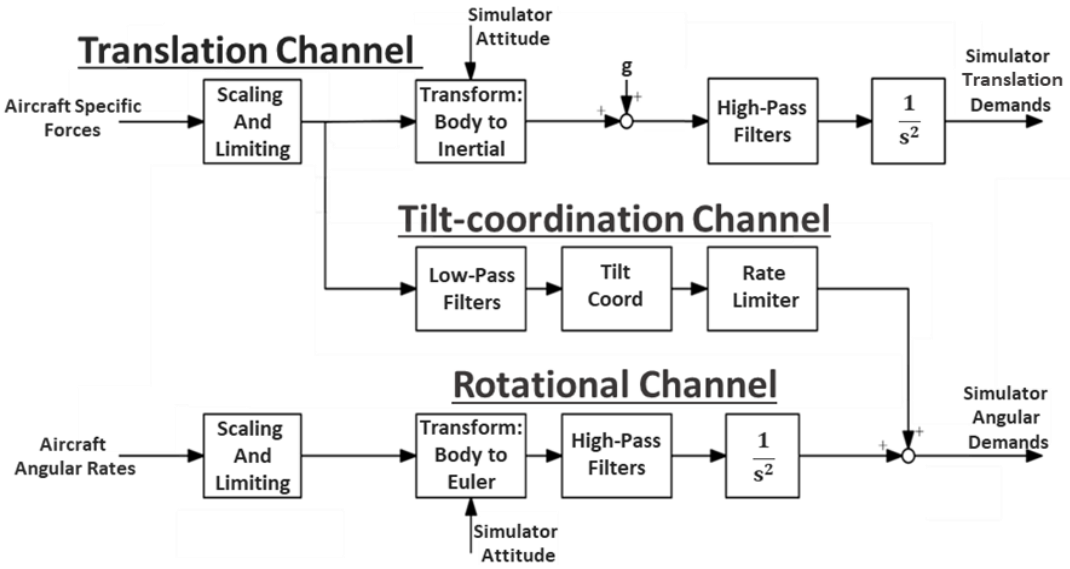

Fig. 4 Classical Washout Algorithm

The CWA obtains aircraft body state information from the flight model and attenuates it to produce simulator motion demands which are then sent to the motion platform actuators. A CWA consists of three channels: translational, rotational and tilt-coordination. Translational and rotational channels each contain three high-pass (HP) washout filters and the tilt-coordination channel contains two low-pass (LP) washout filters. The quantity and the quality of the motion attenuation depends upon the tuning of the HP and LP filter coefficients: gains 'k' and washout or break frequencies 'ω_n', which alter the motion base's response, hence changing the overall behaviour of the motion platform [34]. Altogether, there are sixteen filter coefficients (k_x, k_y, k_z, k_p, k_q, k_r, k_{tilt_x}, k_{tilt_y}, ω_x, ω_y, ω_z, ω_p, ω_q, ω_r, ω_{tilt_x}, ω_{tilt_y}) and the combination of these in all six axes within all three channels forms a Motion Tuning Set (MTS).

The inputs to the MDA are simulated aircraft specific forces per unit mass 'F_{AA}' (excluding gravitational forces) acting at the aircraft's centre of gravity, and aircraft angular rates 'ω_{AA}' as shown in Fig. 4, calculated by, in this case, a helicopter flight model, which, in this study, was a generic FLIGHTLAB model configured to represent a SH-60 Seahawk [36]. The HP filter allows the high-frequency signals to pass through whilst removing the low-frequency signals, which in the translational and rotational channel are sustained motions, translational specific forces and angular rates, that would result in a simulator actuator reaching its motion envelope limit. The HP filter in the translational and rotational channels is a 3rd order filter which provides the washout characteristics that results in returning the platform to its neutral position after an initial onset motion cue has been provided [37]. The LP filters in the tilt-coordination channel allows the low-frequency signals (sustained aircraft specific forces) which were rejected by the HP translational channel to pass through it producing additional specific forces. However, it is important that the pilot does not sense that this sustained translational motion sensation is provided via an angular displacement (tilt) of the simulator. Therefore, the channel is rate limited at between 2-3 deg/s to keep the angular rate (roll/lateral and pitch/longitudinal) below the human perception threshold [38]. The main purpose of the tilt-coordination is to provide a sustained translational acceleration sensation which cannot be provided directly due to constrained simulator motion envelope and makes use of the Somatogravic illusion [39]. Finally, the angular displacement output obtained from the LP channel is added to the HP rotational output to obtain total simulator angular displacement demands, as shown in Fig. 4.

Several studies have been conducted on motion cueing optimisation for flight and driving simulators. Existing literature on motion cueing has proposed different strategies for its assessment and optimisation, potentially using frequency domain techniques (e.g., Sinacori/Schroeder criteria) [40,41], pilot subjective opinion tuning technique,

which is a non-systematic time-consuming approach using pilot-in-the-loop simulations [22,23], and Genetic Algorithms (GA) using fitness functions [24,27,28,42].

The Sinacori criteria is one of the widely used methodologies to potentially assess the fidelity of the simulator motion cueing based on frequency domain characteristics of the washout filters. The Sinacori criteria evaluate the attenuation and phase shift of the washout filter transfer functions at 1 rad/s (the frequency at which the human vestibular system SCC is most sensitive), for translational and rotational channels, separately. The Sinacori fidelity chart is divided into three fidelity regions, i.e., high, medium and low motion cueing fidelity, and was developed through subjective pilot assessments obtained from a brief study conducted in the NASA Flight Simulator for Advanced Aircraft (FSAA) [40]. Sinacori's criteria have continued to be an important baseline metric used by researchers for preliminary motion fidelity observations. The criteria were later refined by Schroeder [41], who also investigated the effect of changes in the visual scene on motion fidelity [43]. Previous studies, e.g., [12], have stated that the high-fidelity boundaries of the Sinacori criteria are unlikely to be met, particularly by small to medium sized hexapod simulators used in academia (actuator stroke < 30 inches), primarily due to the translational motion envelope constraints. However, in the same study, it was found that by carefully harmonising the motions in different axes of a simulator with a modest excursion envelope, representative motion cues can be obtained that improve the pilot's task performance; this is also demonstrated in the present paper.

Grant and Reid [44] developed an expert motion tuning system called 'PROTEST', which transforms subjective pilot comments into a motion parameter tuning. Grant [45] also conducted a simulator study using the University of Toronto Institute for Aerospace Studies' (UTIAS) flight simulator, which focused on reducing the effect of errors in the simulator cueing system and aimed at confirming Schroeder's findings [41]. Hodge et al. investigated yaw and roll-sway motion cues in a short stroke hexapod motion platform using subjective and objective analysis techniques [25,26] and reported that high fidelity motion cueing could be provided by a small to medium motion platforms as well. Hosman et al. [46] introduced a pilot-model based advanced motion tuning procedure based on the analysis of the pilot-vehicle control loop between pilot-aircraft and pilot-simulation models. The technique was utilised to determine the optimised washout filter parameters, restoring the pilot-simulation model control behaviour close to that obtained in real flight.

A method for the objective motion fidelity assessment of flight simulators, the Objective Motion Cueing Test (OMCT) has also been proposed in ICAO 9625 [47], which defines the requirement for robotic testing of flight

simulator motion platforms. It was developed from tests on fixed-wing aircraft simulators and is performed in the absence of the pilot and real-world tasks to develop a set of motion acceptance boundaries [48]. Zaal et al. conducted a series of task-performance based motion cueing pilot-in-the-loop experiments in the NASA VMS flight simulator using different motion configurations to validate the OMCT fidelity boundaries for its use in the commercial transport aircraft [49-52]. The study developed new objective motion cueing boundaries which were mostly obtained within previous boundaries defined in [48]. An OMCT was also conducted on UoL's rotorcraft simulator by Jones et al. [24], which showed a mismatch between the obtained test results and OMCT fidelity acceptance boundaries [47], suggesting that the fixed-wing OMCT boundaries are not directly transferable to rotorcraft applications and, therefore, further rotorcraft related motion fidelity research is required. In Jones et al.'s study, piloted simulations were conducted for motion cueing optimisation for ADS-33E-PRF Mission Task Elements (MTEs) [53] and a proposed surrogate land-based maritime task [54]. The results, however, showed a disagreement between subjective motion fidelity assessments and the OMCT acceptance regions [47].

Recently, automatic GA-based motion tuning techniques have been used for motion parameter optimisation. The GA is a stochastic algorithm which uses a heuristic approach to solve a motion optimisation problem by minimising a fitness function. Casas et al. [39] demonstrated the application of a GA for determining the best motion cues using a simulated virtual motion platform. Asadi et al. [42] introduced an optimal MDA for driving simulators based on a GA approach and non-linear filtering. Jones [24,27,28] used a GA to enhance the motion cues in rotorcraft simulators and conducted flight trial experiments to demonstrate a correlation between GA results and subjective pilot assessments; the results have been encouraging.

CWAs, are widely used in civil and research simulators because of their simplicity. One downside of the use of CWAs has been that they do not consider human perceptual modalities, which should be considered to objectively optimise/tune the motion reproduction in order to provide the "best possible" motion cues to a pilot flying a task in a flight simulator [55]. Song et al. [56] proposed a fuzzy-logic based CWA tuning technique which, in real-time, adjusts the filter cut-off frequencies based on aircraft-simulator states error minimisation in a driving simulator. Sivan, et al. [57] proposed a new MDA which uses a Linear Quadratic Regulator based optimal control technique to obtain linear higher order washout filters using human motion perception models. The technique utilises a cost function that reduces the pilot sensation error between the simulated vehicle and the simulator. This Optimal Algorithm has been implemented by Reid and Nahon in their UTIAS flight simulation studies [30,58]. Later, Telban and Cardullo [59]

proposed a novel real-time approach to the motion cueing which combined the linear Optimal Algorithm with a nonlinear Adaptive Algorithm and incorporated their new integrated human perception model to obtain a set of higher order non-linear washout filters, implemented in NASA Langley Visual Motion Simulator.

However, most of these motion optimisation studies have primarily focused upon single/multi-axis land-based tasks and are typically undertaken in the absence of external factors such as an unsteady airwake and landing spot movement, which are significant fidelity elements in the HSDI environment [1-15]. As will be demonstrated later in this paper, in HSDI operations unsteady aerodynamic forces act upon the helicopter due to the airwake produced by the wind over and around the ship's deck and superstructure, which the pilot needs to compensate for in order to perform the required landing task successfully. The inclusion of such effects on motion fidelity has not been fully examined in the literature. Therefore, the results obtained from the land-based research cannot be directly transferred to the full-axis maritime operations. Further research is required to assess the motion fidelity characteristics and fidelity requirements of simulator motion drive laws for HSDI applications; this paper addresses this requirement.

The paper reports the results of motion cueing research that has been conducted to optimise the motion drive laws specifically for HSDI operations. To objectively assess and optimise the simulator motion cues and determine high fidelity motion cueing for HSDI operations, an offline heuristic approach, the Vestibular Motion Perception Error (VMPE) technique, has been developed which is based on a task-specific vestibular motion perception error minimisation strategy. VMPE integrates vestibular motion perception models with the CWA to quantify the difference, or "error", between the vestibular motion perceived by the pilot in the simulator and in the simulated aircraft, for a particular task using the pilot-in-the-loop simulations. This error is minimised for the purpose of motion cueing optimisation using a trade-off CWA filter parameters ('k' and 'ω_n') tuning strategy.

III. Motion Optimisation: Methodology

The VMPE optimisation approach is based on the concept and objective of minimising the estimated error between the vestibular motion perceived by the pilot in the flight simulator and the simulated aircraft (i.e., flight dynamics model) by tuning the CWA parameters to produce an optimal motion platform setting. Flight simulators, due to the physical design limitations of their motion platform, cannot completely reproduce the sustained accelerations of aircraft; they can only provide the illusion of real aircraft motion to the simulator pilot, primarily through onset cueing. Therefore, it is important to tune the motion system with a formal and rational methodology which provides a reliable measure of the simulator motion fidelity. The motion optimisation process began with the development of a

Matlab/Simulink model to represent the MDA structure of the UoL's simulator. This allowed many MTSs to be evaluated during the offline optimisation process, i.e., prior to real-time piloted simulations.

UoL's FS&T research group operates a fully reconfigurable research simulator, HELIFLIGHT-R (Fig. 5), for the purpose of analysing flight handling qualities, pilot workload assessment, flight model development and simulation fidelity requirements for land-based and maritime operations. Acceptance and commissioning of the simulator was completed in 2008 [22].

Fig. 5 UoL's HELIFLIGHT-R simulator (foreground)

The simulator has been utilised for a wide range of research projects and for undergraduate Aerospace Engineering research and teaching activities [60]. It consists of a 12 ft diameter visual dome mounted on a 6-DOF short stroke Moog hexapod motion system. The simulator uses three high-resolution 2560x1600 WQXGA projectors providing a field of view horizontally of 220° and vertically of 70°. The limits of the HELIFLIGHT-R simulator motion platform are shown in Table 1 [22].

Table 1 HELIFLIGHT-R simulator motion capability [22]

Axis	Displacement	Velocity	Acceleration
Pitch	-23.3°/25.6°	±34°/s	300°/s^2
Roll	±23.2°	±35°/s	300°/s^2
Yaw	±24.3°	±36°/s	500°/s^2
Heave	±0.39 m	±0.7 m/s	±1.02 g
Surge	-0.46/0.57 m	± 0.7 m/s	±0.71 g
Sway	±0.47 m	±0.5 m/s	±0.71 g

The model for the VMPE technique was developed and incorporated within a CWA developed in Matlab/Simulink, as shown in Fig. 6. The combined system consists of four sub-systems: HELIFLIGHT-R MDA, actuator kinematics,

motion centroid transformation and the vestibular motion perception models defined by Telban and Cardullo [59]. The VMPE technique uses a five-step process for determining the optimal MTS for the desired task. The input to the system is the same as the input to the MDA (i.e., the aircraft specific forces and angular velocities), calculated by the vehicle model during the piloted simulation flight trial, and the output from the system is the new MTS with the VMPE value to predict the motion cueing fidelity. The lower the VMPE value, the better the motion cueing fidelity. The system has a dedicated simulator actuator excursion limit indicator which helps to derive a MTS that constrains the HELIFLIGHT-R simulator platform within its motion envelope.

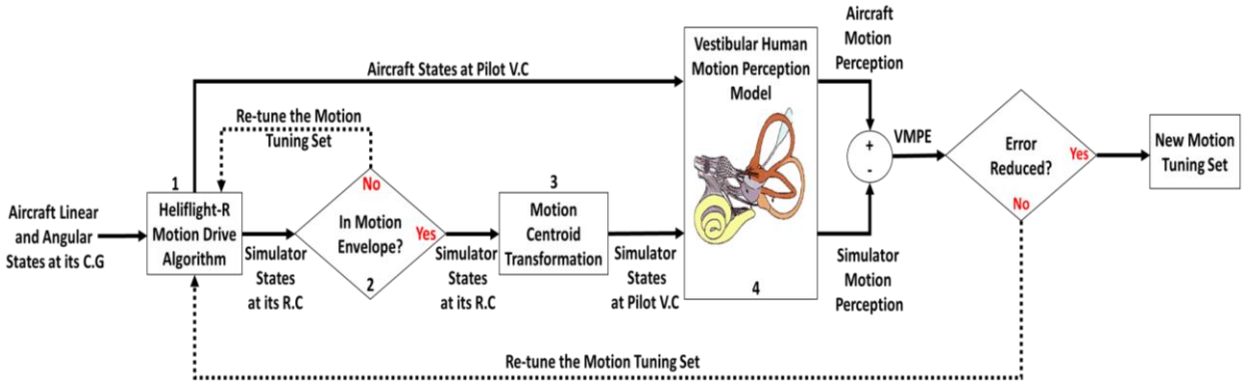

Fig. 6 VMPE technique architecture

The process begins with the input of the simulated aircraft body states obtained from the aircraft model and calculates the simulator inertial motion demands at its Rotational Centre (RC) using the CWA. The aircraft linear body accelerations (a_x, a_y, a_z) are first transformed into the specific forces F_{AA} per unit mass (excluding gravitational forces) acting on the aircraft at its centre of gravity (c.g.) using Eq. (1). These specific forces, along with the angular velocities ω_{AA} of the aircraft (p, q, r), are input to the HELIFLIGHT-R MDA, as shown in Fig. 6.

$$F_{AA} = \begin{pmatrix} f_{xAA} \\ f_{yAA} \\ f_{zAA} \end{pmatrix} = \begin{pmatrix} a_x \\ a_y \\ a_z \end{pmatrix} - \begin{pmatrix} g_x \\ g_y \\ g_z \end{pmatrix} = \begin{pmatrix} \dot{u} \\ \dot{v} \\ \dot{w} \end{pmatrix} - \begin{pmatrix} r \\ p \\ q \end{pmatrix} \begin{pmatrix} v \\ w \\ u \end{pmatrix} + \begin{pmatrix} q \\ r \\ p \end{pmatrix} \begin{pmatrix} w \\ u \\ v \end{pmatrix} - g \begin{pmatrix} -sin\Theta \\ sin\Phi cos\Theta \\ cos\Phi cos\Theta \end{pmatrix} \quad (1)$$

The aircraft specific forces, F_{AA}, before being passed through the scaling block and washout filters to calculate simulator motion demands, are first transformed to the location which physically corresponds to the motion centre of the HELIFLIGHT-R simulator RC using Eq. (2), see Fig. 7. The aircraft specific force vector at this point is denoted as F_{RC}.

$$F_{RC} = F_{AA} + \omega_{AA} \text{ x } (\omega_{AA} \text{ x } R) + \omega'_{AA} \text{ x } R \quad (2)$$

where ω_{AA} is the aircraft angular velocity vector and R is the position vector between the aircraft's c.g. and simulator's RC.

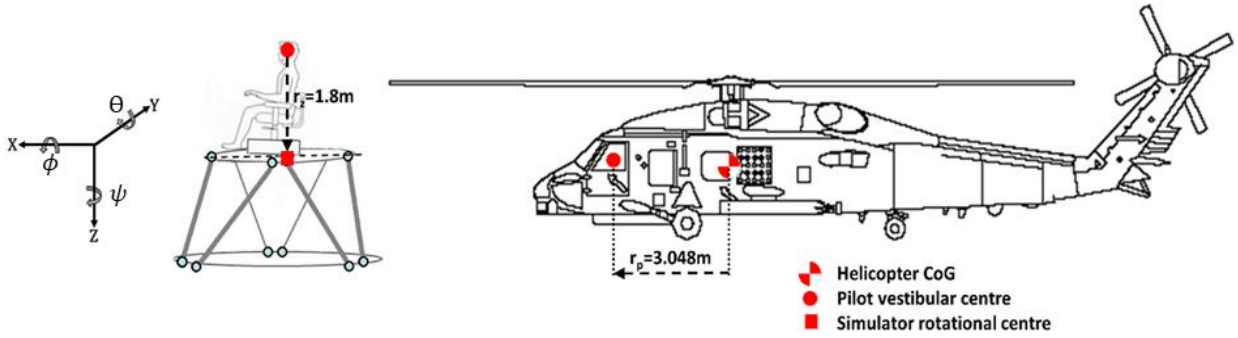

Fig. 7 Motion centroid transformation between helicopter model and simulator (SH-60B configuration)

These forces, F_{RC}, are scaled and limited first and transformed into the inertial frame, and then passed through the HP translational washout filters to obtain simulator translation demands. Similarly, in order to obtain simulator angular demands, $\omega_{s,}$ the aircraft angular rates ω_{AA} are scaled and limited first and transformed into Euler angle rates, and then passed through HP rotational washout filters.

The next step is to determine the simulated aircraft and simulator states at the VC of the human pilot (i.e., at the pilot's ear). This is required because the human senses physical body motion through the vestibular system present in the ear, which is approximately 1.8 m above the RC of the HELIFLIGHT-R simulator, denoted by $r_{z,}$ and 3.048 m ahead of the c.g. of the aircraft, denoted by r_p, in Fig. 7 [12]. Eq. (3) is used to obtain the aircraft specific forces at the pilot position:

$$F_{A\_P} = F_{AA} + \omega_{AA} \text{ x } (\omega_{AA} \text{ x } r_P) + \omega'_{AA} \text{ x } r_P \tag{3}$$

To determine the simulator specific forces at the pilot position, the simulator motion demands obtained at the output of the CWA within the first step are transformed to the specific forces, (f_{xs_RC}, f_{ys_RC}, f_{zs_RC}) at the RC of the simulator using Eq. (4).

$$F_{s\_RC} = \begin{pmatrix} f_{xs\_RC} \\ f_{ys\_RC} \\ f_{zs\_RC} \end{pmatrix} = \begin{pmatrix} a_{xs} \\ a_{ys} \\ a_{zs} \end{pmatrix} - \begin{pmatrix} g_{xs} \\ g_{ys} \\ g_{zs} \end{pmatrix} = \begin{pmatrix} \dot{u}_s \\ \dot{v}_s \\ \dot{w}_s \end{pmatrix} - \begin{pmatrix} r_s \\ p_s \\ q_s \end{pmatrix} \begin{pmatrix} v_s \\ w_s \\ u_s \end{pmatrix} + \begin{pmatrix} q_s \\ r_s \\ p_s \end{pmatrix} \begin{pmatrix} w_s \\ u_s \\ v_s \end{pmatrix} - g \begin{pmatrix} -sin\Theta_s \\ sin\Phi_s cos\Theta_s \\ cos\Phi_s cos\Theta_s \end{pmatrix} \tag{4}$$

In Eq. (4) the accelerations and velocities represent the simulator states in the simulator body frame, whereas Eq. (1) represented the aircraft states. Next, the simulator specific forces at the pilot VC in the simulator, F_{s_P}, are calculated by using Eq. (4) in Eq. (5):

$$F_{s\_P} = F_{s\_RC} + \omega_s \text{ x } (\omega_s \text{ x } -r_z) + \omega'_s \text{ x } -r_z \quad (5)$$

where $-r_z$ is the position vector from the RC of the simulator to the VC of the pilot in the simulator **(**see Fig. 7).

Finally, the specific forces at the pilot's VC in the simulated aircraft and in the simulator are obtained. The angular velocities do not need position transformation since they are independent of the location on the body where they are applied.

In the next step, the perceived specific forces and angular velocities sensed by the pilot's vestibular system in the simulated aircraft and the simulator are calculated by utilising the actual specific forces (F_{A_P} and F_{s_P}) and angular velocities (ω_{AA} and ω_s) in the simulated aircraft and the simulator, calculated in the previous step. This is achieved using the vestibular system dynamics transfer functions (Eqs. (6) and (7)) [59]. Since the vestibular system has two parts, SSC and Oto for angular velocity and linear specific force sensation, respectively, two different models are used to simulate the human vestibular sensory dynamics.

A transfer function of the Otoliths which links the perceived specific force output to actual specific force input is given as follows [59]:

$$\boldsymbol{TF_{OTO}(s) = 0.4\frac{10s+1}{(0.08s^2+5.016s+1)}} \quad (6)$$

A Semi-Circular Canal model transfer function which links perceived angular velocity output to actual angular velocity input is given as follows [59]:

$$\boldsymbol{TF_{SCC}(s) = 5.73\frac{80s^2}{(458.34s^2+85.73s+1)}} \quad (7)$$

The estimated specific force and angular velocity perception in the simulated aircraft and in the simulator are then compared with each other to calculate the VMPE (i.e., motion perception error/deviation) between them. The VMPE gives the measure of the motion cueing fidelity in the flight simulator by calculating the Root Mean Square Error (RMSE) between them, using the Eqs. (8) and (9):

$$RMSE_{VMPE\_Fi} = \sqrt{\frac{\sum_{k=1}^{N}(F_{Ai\_Per} - F_{Si\_Per})^2}{N}} \text{ (ft/s}^2\text{)} \quad (8)$$

$$RMSE_{VMPE\_\omega i} = \sqrt{\frac{\sum_{k=1}^{N}(\omega_{Ai\_Per} - \omega_{Si\_Per})^2}{N}} \text{ (deg/s)} \quad (9)$$

Where i corresponds to the (x, y, z) axis, N is the length of the data vector, F_{A_Per} and F_{S_Per} are perceived specific forces and ω_{A_Per} and ω_{S_Per} are perceived angular velocities, in the simulated aircraft and flight simulator, respectively. The RMSEs of motion perception errors are calculated individually for each axis within each channel (translational and rotational) separately using the above equations and averaged to determine the VMPE for a motion tuning set using Eqs. (10) and (11).

In the cases where the tasks under examination have dominant motion axes belonging to the same channel, i.e., rotational (pitch, roll and/or yaw) or translational (surge, sway and/or heave), then the VMPE of the MTS can simply be obtained by taking the average of the RMSEs of the dominant axis, as an intermediate approach considering a balanced contribution of each dominant axis, using Eqs. (10) and (11).

$$VMPE_{RMSE\text{-}MTS\text{-}f} = \frac{\sum_{k=1}^{m}(\boldsymbol{RMSE_{VMPE\_Fi}})}{\boldsymbol{m}} \ (\text{ft/s}^2) \tag{10}$$

$$VMPE_{RMSE\text{-}MTS\text{-}\omega} = \frac{\sum_{k=1}^{m}(\boldsymbol{RMSE_{VMPE\_\omega i}})}{\boldsymbol{m}} \ (\text{deg/s}) \tag{11}$$

where m is the number of dominant axes.

The primary fidelity objective of the flight simulator motion system is to provide initial onset accelerations to the pilot flying the simulator which are representative of the real helicopter. Therefore, using the VMPE methodology, motion cueing optimisation is achieved by improving the motion platform demands/responses via tuning/adjusting the parameters (k and ω_n) of the CWA filters with an objective of minimising vestibular motion perception error, VMPE, in the channels of interest, while keeping the simulator actuator excursion constrained within its motion envelope (i.e., 0.6 m actuator stroke, Table 1). The application of VMPE is detailed in the next section.

IV. VMPE Application

The VMPE technique was utilised to optimise the motion cueing in the HELIFLIGHT-R simulator, and was accomplished in three phases: pre-validation, pre-trial optimisation and simulated flight trial experiment. In the pre-validation phase, MTSs experimentally tested in a previous motion-dedicated flight trial experiment conducted in HELIFLIGHT-R were acquired, along with the corresponding simulated aircraft accelerations and motion fidelity subjective ratings provided by the test pilot. Subsequently, offline VMPE results were calculated using the VMPE technique for the same MTSs and the results were compared and correlated with the pilot's subjective ratings obtained

during the previous flight trial. This phase was performed to gain confidence in the utilisation of the VMPE technique for offline motion optimisation.

In the pre-trial optimisation phase, the offline VMPE technique was utilised to derive new MTSs for the deck landing task of an SH-60B (Seahawk) simulated helicopter model to a single-spot ship that was based upon a 152 m long UK Royal Navy Type-45 Destroyer (illustrated later in Fig. 24). The simulated aircraft accelerations required to perform the VMPE motion cueing optimisation were acquired from a database of previous flight trial experiments performed in the HELIFLIGHT-R using the baseline motion configurations for different airwake wind conditions and corresponding sea states and ship motion [14].

Finally, in the third phase, a new piloted simulation flight trial experiment was conducted for the same deck landing task using the same HSDI conditions to test the new MTSs obtained in the offline pre-trial optimisation phase and to subjectively examine the vestibular motion cueing fidelity and validate the VMPE predictions. The VMPE application procedure within all three phases is detailed in the following sections.

A. Phase I: Pre-validation

The pre-validation phase consisted of calculating the VMPEs for the MTSs obtained from a previous land-based piloted simulation motion trial experiment conducted by Jones et al. in the HELIFLIGHT-R using a Bell-412 FLIGHTLAB simulated helicopter model [24], which provided specific single-axis and multi-axis cueing demands. The simulator's motion characteristics were examined in the specific dominant axes of the mission tasks within this experiment as follows.

MTSs tested during two ADS-33E-PRF MTEs, Lateral Reposition and Pirouette [53], and a surrogate land-based maritime task, Superslide [54], were acquired from Jones et al.'s experiment [24], along with the corresponding simulated aircraft accelerations recorded during the flight trial. In all these tasks, the dominant axes were from the angular channel in which the motion parameter tuning was undertaken (e.g., roll and pitch in the Superslide task), while motion filter parameters in other non-dominant axes remained constant. The purpose was to examine the congruency between the VMPE (offline objective assessment) estimations and Overall Motion Fidelity Rating (subjective assessment) results obtained from the flight trial, to assess the viability of the VMPE technique for its use in future offline pre-trial simulator motion assessment and optimisation.

The rating scale used to obtain the Overall Motion Fidelity Rating (OMFR) in the flight trial experiment was proposed by Jones et al. [61], shown in Fig. 8. The scale is a 5-point rating scale, 1(Good) to 5(Poor) and classified

into three coarse levels: high, medium and low motion cueing fidelity. The fidelity levels of the scale are inspired by the descriptions of the Sinacori/Schroeder motion boundaries [40,41]. The OMFR scale helps the pilot assess the motion cueing errors first in dedicated axes followed by a rating of the overall MTE. The scale is more relevant and prominent to the specific MTE task applications.

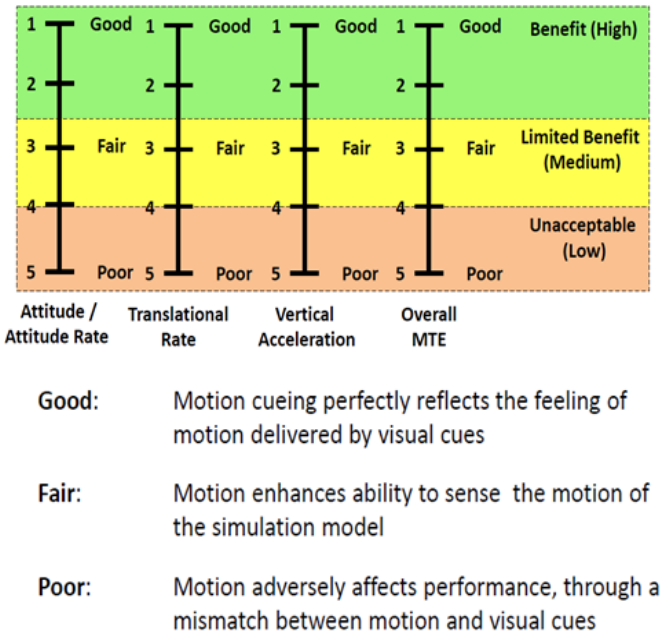

Fig. 8 OMFR scale [61]

1. Case I: Superslide Task

The Superslide task is a land-based task aimed at representing a shipborne landing flight test manoeuvre and contains elements of the station-keeping requirements apparent in deck landings [54]. In the motion cueing optimisation study, only the hover portion of the overall task was examined. The hover element of the task required tracking of a moving black hover board (see Fig. 9), which is driven horizontally and vertically to replicate the motion of the ship's landing deck. In the experiment, it represented the motion of a frigate in a Sea State (SS) 4 condition and constitutes a pursuit tracking task where the target (i.e., the hover board) is independently moving [1].

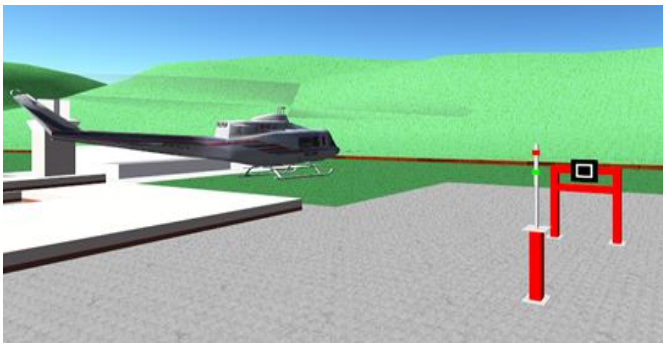

Fig. 9 Superslide MTE course in HELIFLIGHT-R simulator

Within Jones et al.'s flight trial experiment [24], motion parameter tuning was undertaken in the roll (p) and pitch (q) axes of the HP rotational channel, while no modifications were carried out in the translational channel, which was configured using HELIFLIGHT-R's default motion settings. Whilst heave is an axis of interest in the Superslide task, the rotational axes were the main axes of interest in this study, rather than translational axes. [54]. Six different MTSs, together with corresponding simulated aircraft accelerations recorded during the flight trial, were acquired to calculate the VMPEs, Table 2.

Table 2 Superslide task MTSs and filter parameters

Filter Parameters	MTS #1	MTS #2	MTS #3	MTS #4	MTS #5	MTS #6
$k_{p,q}$	0.6	0.4	0.4	1.0	0.6	0.8
$\omega_{p,q}$	1.0	0.6	0.3	1.4	0.6	1.2

These MTSs are plotted on the Sinacori chart in Fig. 10, which defines the high, medium and low motion fidelity boundaries. Each of the coloured dots plotted on the chart represents a unique combination of the motion filter gains and washout frequencies. The comparison of the results obtained from the VMPE offline test and OMFR subjective experiment for different MTSs is shown in Fig. 11.

Comparison of the VMPE estimations with the OMFR ratings shows that the two correlate well, and that out of all the MTSs tested, MTS#3 was awarded the lowest OMFR rating and the VMPE estimate was minimum as well, suggesting it provided the best motion cues to the pilot. MTS#4 was awarded the highest OMFR and the VMPE was estimated to be highest as well, suggesting this provided the worst motion cues. The Sinacori chart, Fig. 10, shows that MTS#3 is closest to the high-fidelity region while MTS#4 is farthest into the low fidelity region.

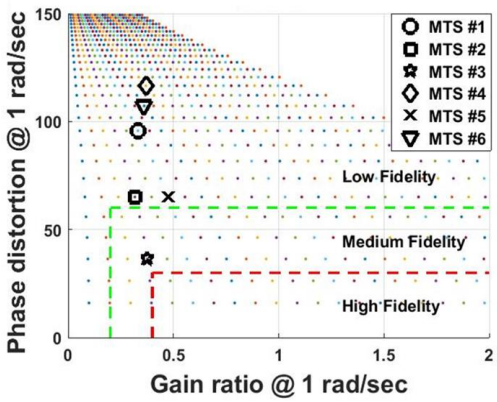

Fig. 10 Sinacori chart (Superslide)

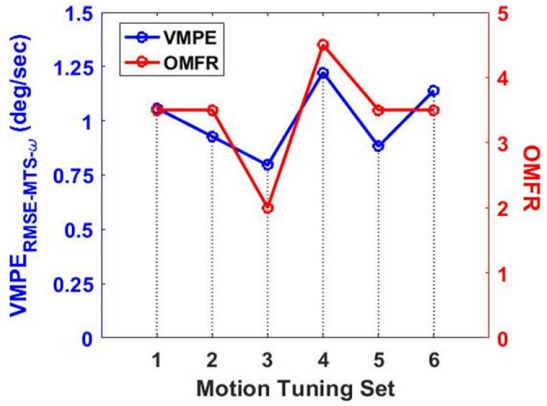

Fig. 11 VMPE and OMFR comparison (Superslide)

2. Case II: Lateral Reposition Task

The ADS-33 lateral reposition task focuses primarily on roll and sway motion characteristics of the aircraft. The task course is shown in Fig. 12. The motion variations were undertaken in the roll axis by tuning 'k_p' and 'ω_p' in the HP rotational channel of the cueing algorithm, while other parameters remained constant using HELIFLIGHT-R's default motion configuration [24]. From a stabilised hover at the left-hand end of the course (position A), the pilot was required to translate the aircraft sideways to the right-hand end of the course (position B), attempting to complete the manoeuvre within the performance limits detailed in ADS-33 [53]. The markings in the hover position (black and red boxes) indicate to the pilot the desired and adequate performance standards, respectively.

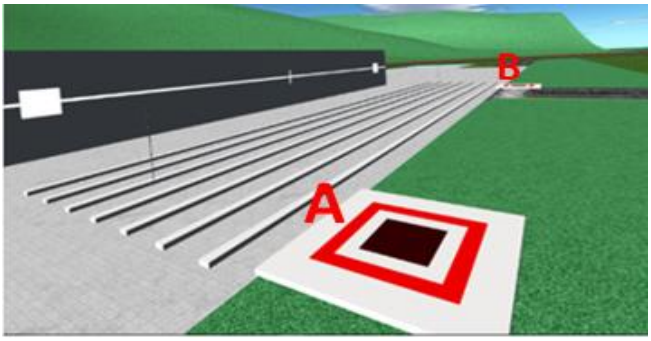

Fig. 12 Lateral Reposition MTE course in HELIFLIGHT-R simulator

A similar pre-validation VMPE application methodology was employed here, as case I. Six different MTSs (Table 3) along with corresponding simulated aircraft accelerations recorded during Jones et al.'s experiment [24] were acquired and examined to calculate the VMPEs for each of the MTSs. Figure 13 shows the MTSs plotted on the

Sinacori chart. Figure 14 shows the comparison of the VMPE estimations with the OMFR ratings for the different MTSs.

Table 3 Lateral Reposition task MTSs and filter parameters

Filter Parameters	MTS #1	MTS #2	MTS #3	MTS #4	MTS #5	MTS #6
k_p	0.2	0.4	0.2	0.3	0.4	0.6
ω_p	0.3	0.3	0.7	0.7	1.0	1.0

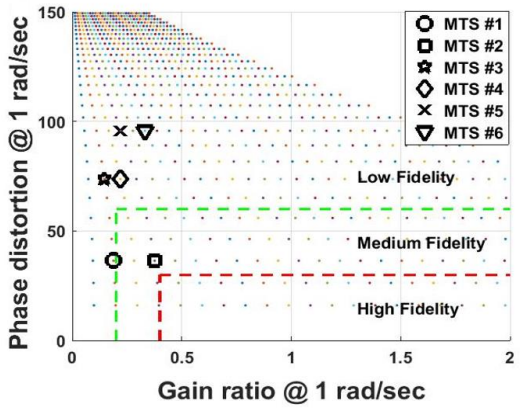

Fig. 13 Sinacori chart (Lateral Reposition)

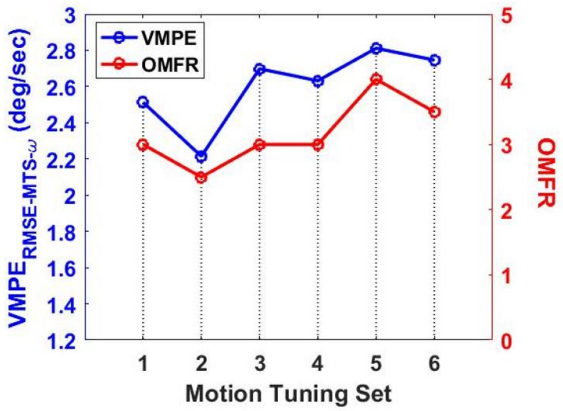

Fig. 14 VMPE and OMFR comparison (Lateral Reposition)

It can be seen from Fig. 14 that the two measures again correlate well. MTS #2 was awarded the lowest OMFR and the VMPE was estimated as minimum. The Sinacori chart shows that this point is closest to the high-fidelity region. On the other hand, MTS #5 was awarded the highest OMFR and the VMPE estimate was highest and, as can be seen from the Sinacori plot, this point is farthest into the low fidelity region.

3. Case III: Pirouette Task

In the Pirouette task, the tuning of the MDA filter parameters was performed in all axes of the rotational channels (i.e., roll, pitch and yaw), the parameters in the translational channel were kept constant at the baseline translational channel configuration of the HELIFLIGHT-R simulator to maintain the balance, as in previous MTE cases [24]. The Pirouette task course can be seen from Fig. 15. The pilot attempts to follow the black track line while facing the central pole; the orange cones and white ground markers provide cueing for the desired and adequate performance standards for the MTE, with height cueing requirements provided by the central pole.

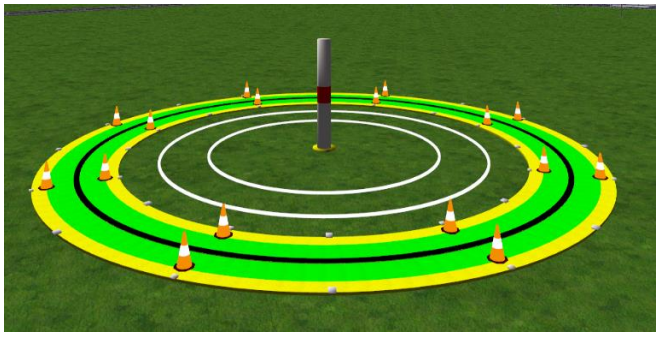

Fig. 15 Pirouette MTE Course in HELIFLIGHT-R Simulator

Using the same VMPE methodology, six MTSs along with the corresponding simulated aircraft accelerations were acquired from the experimental data [24], see Table 4.

Table 4 Pirouette task MTSs and filter parameters

Filter Parameters	MTS #1	MTS #2	MTS #3	MTS #4	MTS #5	MTS #6
$k_{p,q,r}$	0.2	0.4	0.4	0.6	0.6	0.6
$\omega_{p,q,r}$	0.3	0.3	0.6	0.6	1.0	1.4

The Sinacori chart in Fig. 16 shows all the six MTSs plotted, the 'k' and 'ω_n' values were kept the same in all the angular axis during the variation. Figure 17 shows the comparison of VMPE and OMFR.

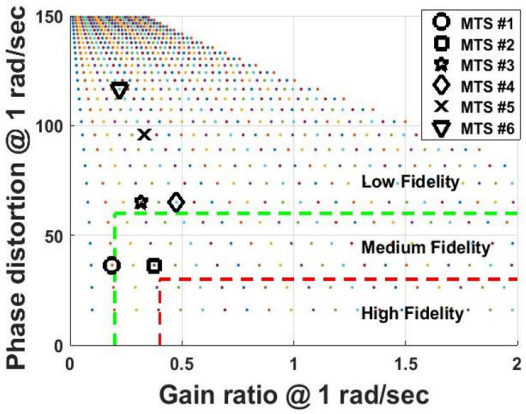

Fig. 16 Sinacori chart (Pirouette)

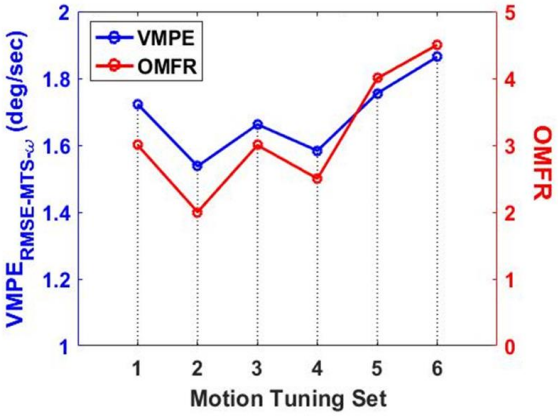

Fig. 17 VMPE and OMFR comparison (Pirouette)

Again, the OMFR and VPME values correlated well and it can be seen from Fig. 17 that MTS#2 was awarded the best OMFR while MTS#6 was awarded the worst OMFR. Comparing it with VMPE estimations, the VMPE for and MTS#2 was lowest and for MTS#6 was highest. The Sinacori chart is again consistent with the results of the VMPE

and OMFR metrics.

From all these pre-validation exercises it can be seen that the VMPE estimations correlate well with the subjective pilot ratings. This provided confidence in using the VMPE technique for future offline optimisations. Therefore, the next step of the VMPE technique was to apply it to the full-axis shipboard landing task to derive the new simulator MTSs by using simulated aircraft accelerations data obtained from a database of previous flight trial experiments conducted in the HELIFLIGHT-R simulator using its default baseline motion configuration.

B. Phase II: Pre-trial Optimisation

The next stage in the process began with the acquisition of FLIGHTLAB SH-60B simulated aircraft accelerations datasets from a ship deck landing flight trial experiment conducted on a single spot naval destroyer at a range of different WOD conditions (detailed in the next section) using the baseline motion filter configuration in the HELIFLIGHT-R [14].

Initially, the baseline MTS was selected from the generic HELIFLIGHT-R configuration and tuning of the CWA filter parameters was performed using the offline VMPE technique to derive new MTSs. The optimisation strategy was to perform a trade-off between gains 'k' and washout frequencies 'ω_n' of the translational and rotational channels of the CWA, with an objective of minimising the overall motion perception error (VMPE) thus improving the motion base's response, while keeping the simulator motion constrained within platform limits. The purpose was to derive new MTSs with a range of motion perception error differences between them to test the sensitivity of the approach when examining the overall performance of the deck landing operations. Using this strategy, four new motion tuning sets (designated as Benign, Intermediate, Responsive and Optimised) were derived for two different wind azimuth conditions, H00 headwind and Green 45 oblique wind (i.e., wind direction relative to the ship 45° off starboard side, G45), at different wind speeds. 'Benign' MTS as its name suggests was predicted to provide the worst motion cues and 'Optimised' the best based on VMPE estimations shown in the next section.

Since in the deck landing operation all platform axes are required for the motion cues and are relevant to the mission task, tuning was performed in all six HP filter channel axes (surge, sway, heave, pitch, roll, and yaw). RMSs of the motion perception errors were calculated individually for each axis and averaged to estimate the mean specific force perception error $VMPE_{\mathbf{RMSE\text{-}MTS\text{-}f}}$ in the translational channel and mean angular velocity perception error $VMPE_{RMSE\text{-}MTS\text{-}\omega}$ in the rotational channel for each MTS and WOD condition, using Eqs. (10) and (11), respectively.

1. Simulated Deck Landings VMPE Application

For the motion cueing optimisation in the simulated shipboard landing task, six HSDI WOD conditions (H00 25, 35 and 45 kts and G45 15, 25, and 35 kts) were examined. Figures 18 and 19 shows the results of the estimated VMPEs for the 24 cases examined, six WOD conditions and four newly derived MTSs (Benign, Intermediate, Responsive and Optimised). Pearson's correlation coefficients (ρ) between the motion perceived in the simulator and simulated aircraft for each of the 24 cases are also shown.

It can be seen from Figs. 18 and 19 that as the VMPE decreases from Benign (Bn) to Optimised (Op) MTS in both channels, linear and angular, the correlation coefficient increases, respectively, for each of the six WOD cases. The Benign motion tuning set was overall predicted to provide the worst motion cueing and Optimised the best. For the most demanding H00 WOD case of 45 kts WOD (red lines), Fig. 18, from Benign to Optimised MTS, the mean specific force perception error $VMPE_{RMSE\text{-}MTS\text{-}f}$ was reduced from 1.46 ft/s^2 to 1.34 ft/s^2, the mean angular velocity perception error $VMPE_{RMSE\text{-}MTS\text{-}\omega}$ was reduced from 2.91 deg/s to 1.95 deg/s and the mean correlation increased from 54.5 % to 71.9 %.

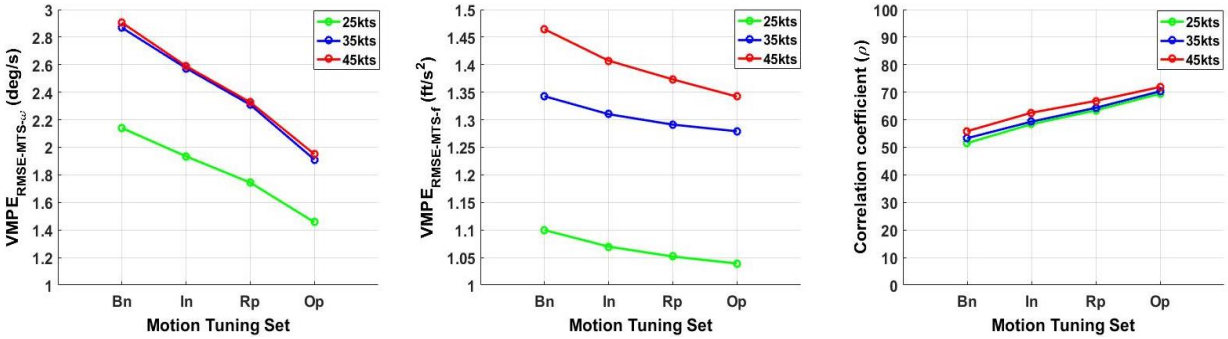

Fig. 18 VMPE estimations for four new MTSs in H00 WOD condition ('Bn' is Benign, 'In' is Intermediate, 'Rp' is Responsive and 'Op' is Optimised)

For the most demanding G45 WOD case of 35 kts WOD (red lines), the mean specific force perception error $VMPE_{RMSE\text{-}MTS\text{-}f}$ was reduced from 1.41 ft/s^2 to 1.29 ft/s^2, mean angular velocity perception error $VMPE_{RMSE\text{-}MTS\text{-}\omega}$ was reduced from 2.73 deg/s to 1.87 deg/s and the mean correlation increased from 48.2 % to 68.1 %, see Fig. 19.

The Sinacori charts, in Fig. 20 shows the HP and LP filter parameters for the four new MTSs. Only four MTSs were derived due to the HELIFLIGHT-R motion excursion limits and the requirement to obtain a sufficient difference in the VMPE estimate between two MTSs in order to allow the pilot to perceive noticeable motion cueing difference/mismatch. For all the tuned cases shown in Fig. 20, it can be observed from the charts that there was more

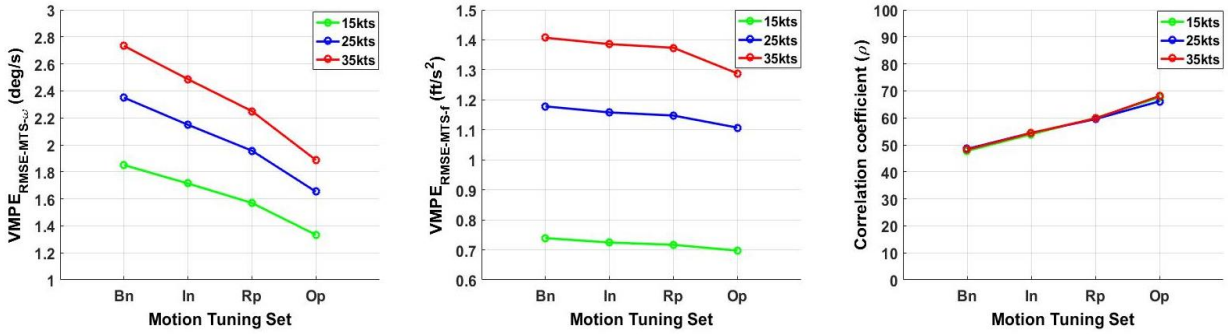

Fig. 19 VMPE estimations for four new MTSs in G45 WOD condition ('Bn' is Benign, 'In' is Intermediate, 'Rp' is Responsive and 'Op' is Optimised)

opportunity to optimise the motion cueing in the angular channel as it would demand a lesser extension of the simulator actuators and hence filter values could be obtained in the "medium to high" motion fidelity regions. This requirement to harmonise motions in different axes was also observed in Hodge's motion experiment [12] and is dependent on the size of the platform motion envelope and the aggressiveness of the mission task under examination. Due to the limits of the motion envelope, the translational channel filter values were obtained in the low fidelity region since it demands greater excursions of the simulator actuators. This can be noticed from the VMPE estimations in Fig. 18 and 19 as well, where the difference in linear channel specific force perception errors $VMPE_{RMSE\text{-}MTS\text{-}f}$ between different MTSs is comparatively smaller than in the angular channel. This is further demonstrated later in Fig. 23.

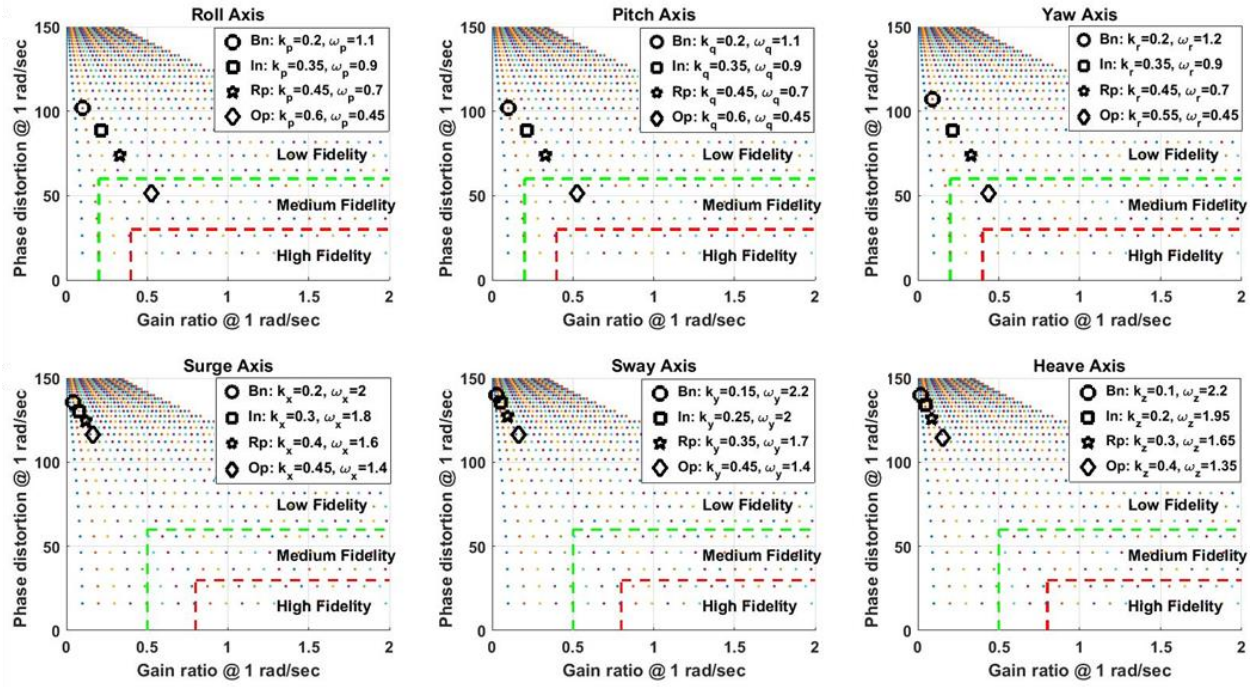

Fig. 20 Four new MTS filter parameters (k and ω_n) plotted on Sinacori chart for each axis ('Bn' is Benign, 'In' is Intermediate, 'Rp' is Responsive and 'Op' is Optimised)

Figures 21 and 22 show the VMPE error (grey area) and correlation between the perceived motion (specific forces f_i-per and angular velocity ω_i-per, calculated using Eqs. (6) and (7)) in the simulated aircraft and flight simulator for the H00 case for which VMPE estimations are shown in Fig. 18. Results from the two extreme cases, H00 45 kts WOD Benign and Optimised MTSs are shown in Figs. 21 and 22, respectively, since these were assumed to provide the maximum cueing difference to the pilot; this was confirmed by the flight trial experimental results in the next section. The grey area between the lines is the error between the simulator and simulated aircraft motion perception (VMPE), which is quantified using the RMS measure (Eqs. (8) and (9)) and thus motion cueing predictions were made on the basis of that. It can be seen that this grey area in the Benign case (Fig. 21) is noticeably larger than the Optimised MTS case (Fig. 22). Moreover, comparing the perceived specific forces and angular velocities motion for the simulator in Figs. 21 and 22 (blue lines), the Optimised MTS has resulted in the simulator motion perception becoming much more dynamic compared with the Benign MTS, hence predicted to potentially provide enhanced motion feedback (e.g., of the external airwake disturbances) to the pilot. This is demonstrated by the flight trial experiment results later in Figs. 31 and 32. Similar results were obtained for the G45 35 kts WOD case.

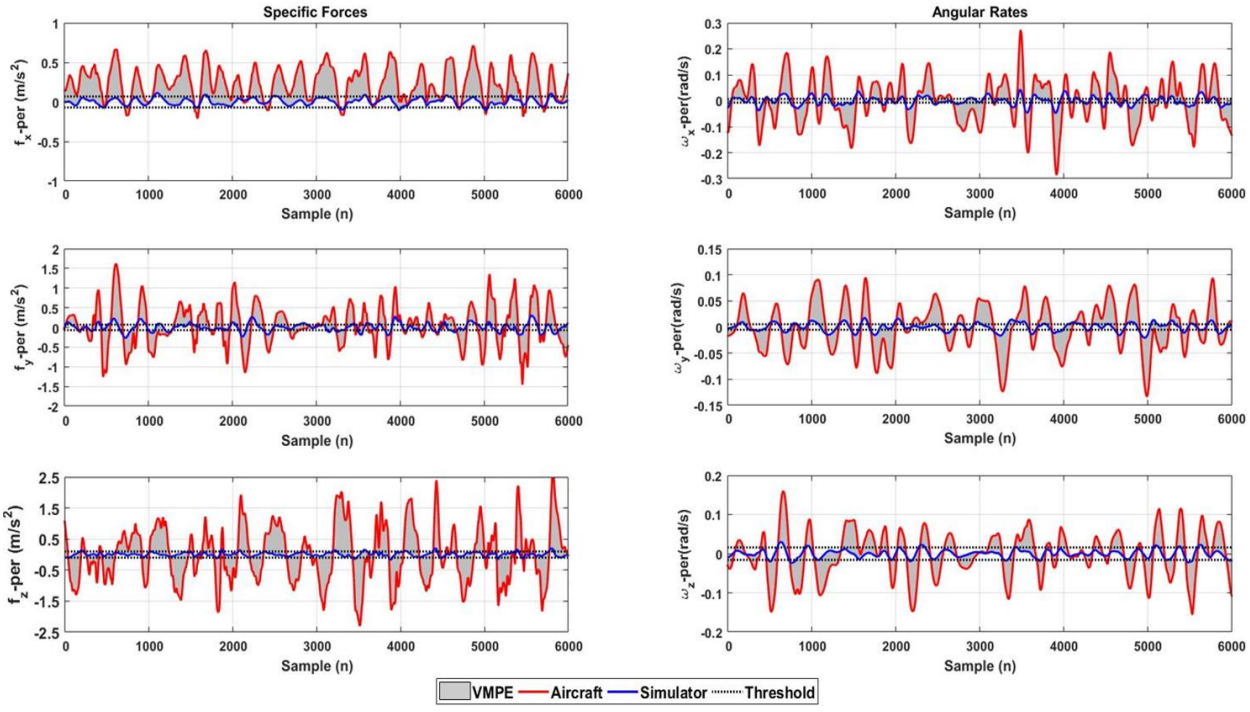

Fig. 21 Comparison of perceived specific forces and angular velocities in the simulated aircraft and flight simulator for Benign MTS case

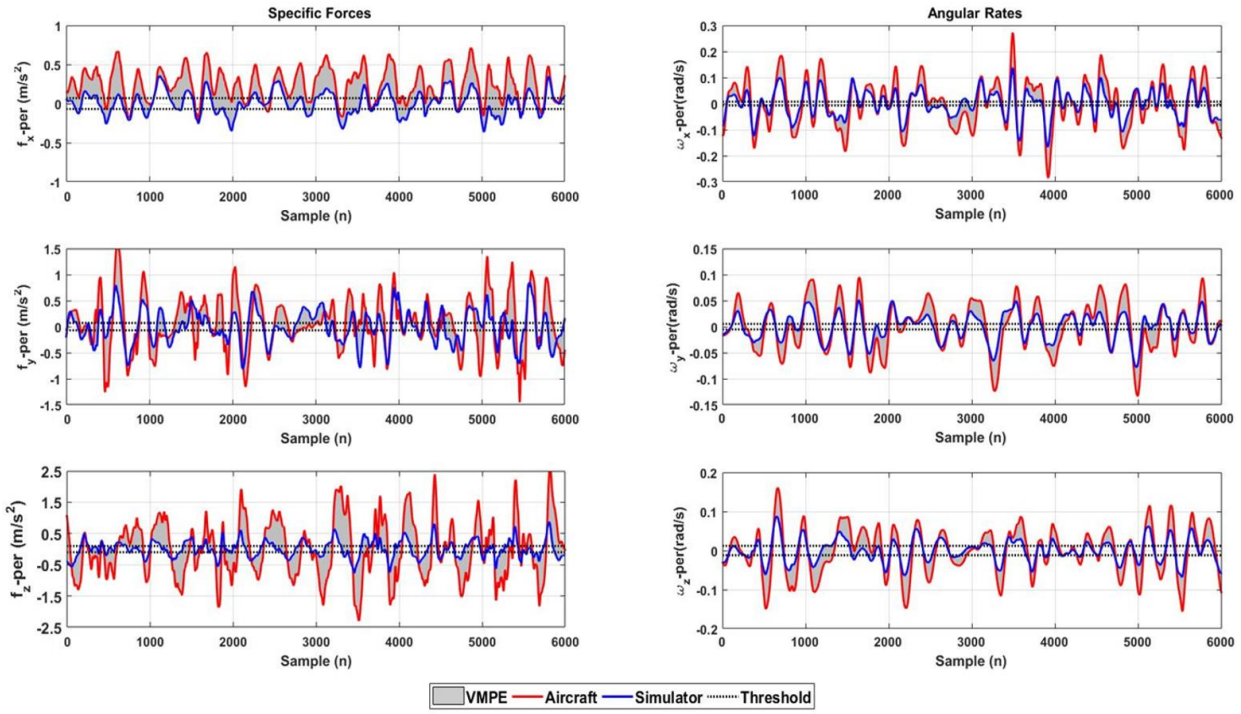

Fig. 22 Comparison of perceived specific forces and angular velocities in the simulated aircraft and flight simulator for Optimised MTS case

During the optimisation process, human motion perception thresholds were utilised to evaluate whether the perceived specific forces and angular rates evaluated using the VMPE for a particular MTS were sub- or super-threshold. Figures 21 and 22 show the perception threshold limits in dotted black lines acquired from a motion perception threshold detection experiment conducted in the SIMONA simulator [62]. The SIMONA limits are 0.0742, 0.0743, and 0.123 m/s^2 for surge, sway, and heave, respectively, and 0.00521, 0.00734, and 0.0166 rad/s for roll, pitch and yaw, respectively [63]. Several studies have been conducted into the measurement of perception thresholds in different environments and task conditions using different systems and techniques. For example, the thresholds obtained in the laboratory experiments with passive subjects are significantly different from the ones obtained in the simulator-based studies. Therefore, there is still some debate regarding the constant and universally accepted values of these thresholds. The values are highly influenced by the simulation environment, equipment used, human subject characteristics, task under examination, manoeuvre and the experimental technique. As observed in the initial phase of this research presented in [64], the worst MTS provided mostly sub-threshold simulator motion perception except for a few instances, but the pilot was able to perceive the physical motion during the flight trial experiment which varied also in different HSDI conditions and MTEs of the deck landing task. This observation has been true for the cases examined in this study as well since more challenging HSDI conditions were simulated. This suggests that

further research is required to determine more representative motion perception threshold limits specifically for simulated operations in dynamic environments, such as the HSDI.

Figure 23 shows the accumulated VMPE results from the pre-trial optimisation phase for the two cases examined, H00 and G45. It can clearly be seen that the Benign MTS is estimated to be the worst MTS and Optimised MTS the best, based on the VMPE calculations in both the cases. Also, the motion perception error increases with the wind magnitude due to more simulator accelerations desired at higher WOD conditions but being constrained due to the limited simulator motion envelope. Moreover, it is evident that from Benign to Optimised MTS the rate of decrease in motion perception errors (VMPEs) in the translational channel is smaller than in the rotational due to translational accelerations demanding greater simulator actuator excursions and therefore less opportunity for improving motion response in the translational channel, as can be seen from Sinacori charts in Fig. 20.

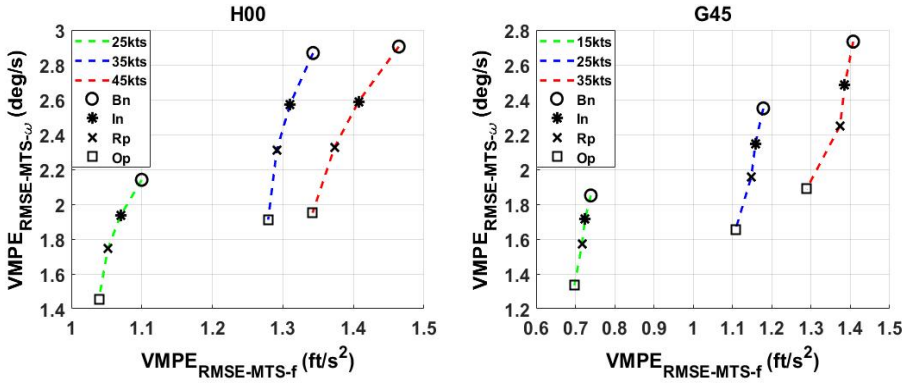

Fig. 23 VMPE estimations for two HSDI tasks (H00 and G45)

C. Phase III: Simulated Flight Trial Experiment

The four new MTSs, derived in the "Pre-trial Optimisation" phase of the VMPE technique application described in the previous section, were deployed and experimentally examined in the HELIFLIGHT-R simulator by an experienced ex-Royal Navy test pilot, who subjectively assessed the motion cueing fidelity in the same six HSDI conditions in ahead and oblique winds (H00 25, 35 and 45 kts and G45 15, 25, and 35 kts) and associated sea states.

In the flight trial experiment, the landing procedure was split into three Mission Task Elements (MTEs) according to the standard UK forward-facing port-side deck landing procedure [2], Fig. 24. MTE 1 consists of a lateral translation from off the port side of the ship across the flight-deck to a position above the landing spot, at a hover height of 30ft. MTE 2 consists of a 30 second period of stabilized hover station-keeping prior to the landing. Finally, MTE 3 is the descent from the hover to touchdown on the flight deck.

Fig. 24 Mission Task Elements (MTEs) of the deck landing task

The motion fidelity was assessed and rated subjectively using the Hodge Motion Fidelity Rating Scale (HMFR), Fig. 25, proposed by Hodge et al. [25]. The rating scale is a 10-point decision tree scale which has the same structure as the Cooper-Harper Handling Quality Rating (HQR) scale. The scale is separated into three coarse levels of high, medium and low motion fidelity, broadly correlating to the three fidelity regions of the Sinacori/Schroeder criteria. These three levels are each further expanded into three more descriptions, which allows the pilot to better describe their perception of the vestibular motion cues, comparing them with real-world motion cues. Moreover, the HMFR scale provides alphabetic suffixes (descriptors) to supplement the numerical ratings to discern any possible motion cueing deficiencies experienced by the pilot. Therefore, the HMFR scale was selected for subjective assessments in the full-axis HSDI task experiment.

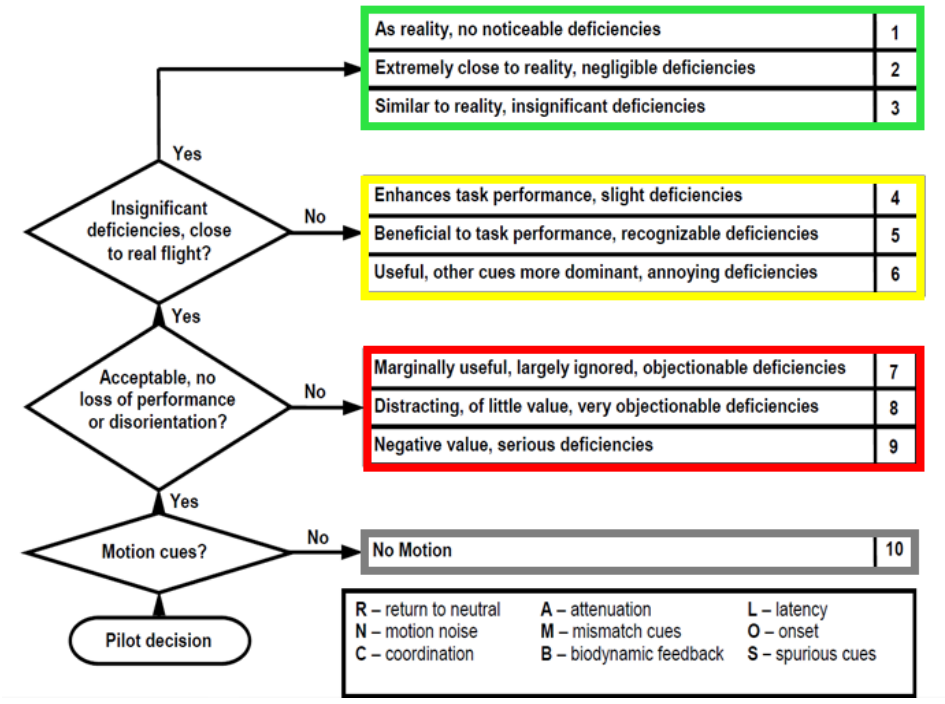

Fig. 25 Hodge Motion Fidelity Rating (HMFR) scale [25]

V. Flight Trial Results

A. Simulated Landing Flight Trial

The simulated flight trial experiment was conducted to examine the flight simulator motion cueing fidelity using the HMFR scale for the four new MTSs derived in the presence of turbulent unsteady ship airwake and corresponding ship motion at a 12 kts forward speed. The piloted simulation flight trial consisted of a test matrix of 24 deck landings at six WOD conditions and using four MTSs, as examined in the "Pre-trial Optimisation" phase (section IV.B). The ship motion was modelled using ShipMo3D, a well-validated ship motion potential-flow code developed at Defence Research and Development Canada (DRDC) – Atlantic and made available to the UoL [65]. The test matrix is shown in Table 5.

Table 5 Piloted simulation flight trial test matrix

S.no	WOD Magnitude	WOD Azimuth	Ship Motion (SS=sea state)
1	25		SS4
2	35	H00	SS5
3	45		SS5
4	15		SS4
5	25	G45	SS5
6	35		SS5

Figure 26 shows the flight trial results for the 24 cases tested. As can be seen, the pilot reported improved motion fidelity ratings as the MTS was progressively tuned. The Benign motion set was subjectively rated worst and the Optimised as best by the pilot, as predicted in the offline optimisation using the VMPE technique, section IV.B.

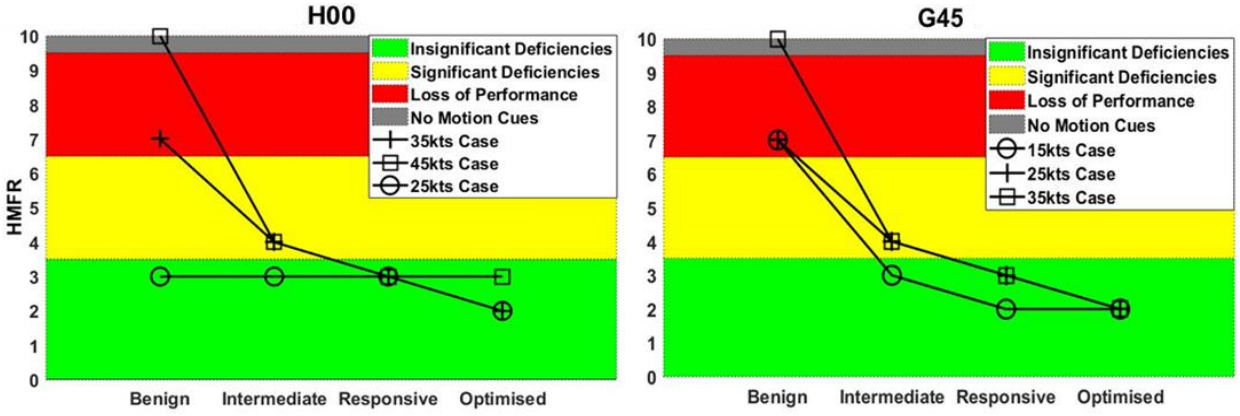

Fig. 26 Flight trial experiment subjective (HMFR) results for H00 and G45 WOD cases

In the H00 case, it can be seen from Fig. 26 that at the 25 kts WOD condition the subjective ratings remained constant (HMFR=3) for the first three MTSs (Benign, Intermediate and Responsive) and decreased to 2 for the Optimised MTS case; this is because at this low wind speed the motion cues obtained from the visual scene (i.e., vection) were sufficient for the pilot to perform the task since there were benign external airwake disturbances. This observation was supported by pilot comments at 25 kts H00: "*More balanced look at visual cues*", "*Able to hold the position due to lower airwake disturbance*" and "*All very smooth due to low WOD wake*". However, using the 'Optimised' MTS case, the HMFR awarded at H00 25 kts case was 2 where the pilot commented: "*Lighter winds but got an impression of wake throughout which was missing before*", "*Felt gust disturbance in hover*" and "*More powerful and harmonized*". This suggests that even though the external disturbances were low at the 25 kts H00 WOD condition and visual motion cues were sufficient for the task performance when the Optimised MTS was used, the overall simulation perception improved because the physical motion complemented the visual cues.

When the WOD magnitude in the H00 case was increased to 35 kts and 45 kts, using the Benign MTS the HMFR increased to 7 and 10 suggesting objectionable motion cueing deficiencies and negative motion cueing, respectively. The pilot commented: "*Very benign motion cueing*", "*Barely perceptible*", "*Poor visual/vestibular synchronisation*", "*Pilot would expect to feel airwake bumps at this WOD condition*", "*Motion cueing is objectionable*" and "*Motion not helpful at all*". These comments correlate with the awarded HMFR suffixes: L (Latency), M (Mismatch) and A (Attenuation). Whereas, the HMFR decreases to 2 and 3, respectively, at the same WOD conditions using the Optimised MTS, suggesting good motion cueing experience with negligible deficiencies. The pilot commented: "*More powerful motion cueing*", "*Accurate linear acceleration cues*", "*More crisp motion cues with translations*", "*Couldn't feel any deficiencies*" and "*Overall reasonable and powerful*".

In the G45 case, using the Benign MTS the HMFR ratings awarded were in Level 3 of the HMFR scale, as shown in Fig. 26, for all the wind speed cases. The pilot commented: "*Very little motion felt*", "*Visual cues were dominant*", "*Not the hardest task but poor motion cues making it difficult*", "*Visual-vestibular mismatch*" and "*Difficult to perform the task accurately, especially hover*". In this case as well, the comments matched with the HMFR suffixes added by the pilot: M (Mismatch) and A (Attenuation). When the same WOD conditions were tested using the Optimised MTS, the HMFR decreased significantly to 2 for all three wind speeds, suggesting much better motion cueing. The pilot commented: "*Visual and vestibular motion harmonised*", "*Decent cueing*", "*Motion cueing positive*", "*Vestibular*

motion positively contributing to overall simulation perception", "*Motion highly harmonised*" and "*Workload decreased*".

Having demonstrated how the Optimised MTS improves the simulation motion fidelity, the next question was how the different levels of motion cueing fidelity would affect pilot workload during a simulated deck landing task. The airflow over the deck is known to be less aggressive in winds from ahead, compared with oblique winds (e.g., Ref. [9]). The reason for this can be seen in Fig. 27 which shows the turbulence intensity in the airwake in a horizontal plane at the height of the ship's hangar for relative winds from ahead and from 45° off the starboard (G45). In the headwind the turbulence in the airflow over the flight deck is relatively uniformly distributed; this is felt, through the main rotor, as a vibration on the aircraft. There will also be a recirculating airflow over the deck in the lee of the hangar. While the airflow over the deck does present challenges to the pilot in a headwind, in the G45 wind the air separates from the vertical starboard corner of the hangar and cuts diagonally across the flight deck. A steep shear layer is formed between the fast-moving unrestricted airflow and the slower moving recirculation behind the hangar. The difference in air speed, as well as the concentrated area of high turbulence, act on the helicopter to create unsteady forces and moments that make it difficult for the pilot to control the aircraft. As will be seen in the following discussion, therefore, pilot workload and control activity will be greater in the G45 WOD case and explains why Table 5 shows that lower wind speeds were used in the G45 WOD tests.

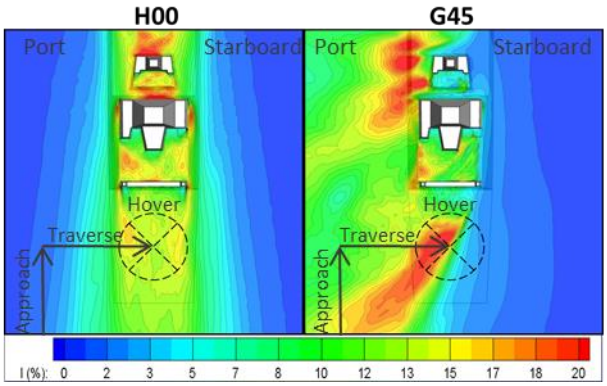

Fig. 27 Turbulence intensity contours for H00 and G45 WOD (at hangar height) [14]

The pilot workload was assessed for each of the three MTEs illustrated in Fig. 24 using the Bedford Workload Rating (BWR) scale [66]; the complete landing task was assessed using the Deck Interface Pilot Effort Scale (DIPES) [2]; the two scales are included in the Appendix. In the 35 kts G45 Benign MTS case, the workload rating provided by the pilot was highest with BWR of 5, 6 and 6 for MTE 1, 2 and 3, respectively. The BWR reduced using the

Optimised MTS to 4, 4 and 3. Similarly, for the 45 kts H00 Benign MTS case, BWR awarded was 2, 5 and 5 for MTE 1, 2 and 3, respectively, which reduced to 2, 3 and 4 using the Optimised MTS.

DIPES ratings obtained from the simulated flight trial results are plotted on the SHOL axes in Fig. 28 for the two extreme MTSs tested, Benign and Optimised. It was observed that, using the Benign MTS, the DIPES awarded by the pilot for G45 35 kts WOD case was 3 which is identified as the limit of the simulated SHOL envelope boundary [3]. However, when the Optimised MTS was used, the DIPES awarded for the same G45 35 kts WOD case was 2. The workload experienced by the pilot, whether measured by the BWR for the different MTEs, or by DIPES for the overall landing task, was therefore affected by the tuning of the simulator motion, particularly in more aggressive winds that generate more dynamic loads on the helicopter. For the tests conducted using the Optimised MTS, which produces the highest fidelity rating, they also lead to lower workload and therefore have a bearing on the accuracy of a simulated SHOL; this shows that inappropriate motion tuning and poor motion cues can adversely affect the ability to satisfactorily predict SHOL boundaries through flight simulation.

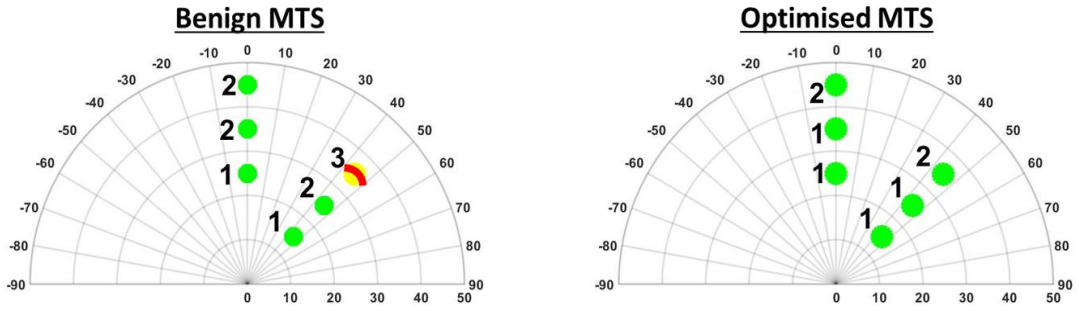

Fig. 28 DIPES ratings for Benign and Optimised MTS plotted on SHOL axis for H00 and G45 WOD cases

Further evidence of the effect of motion tuning on the pilot's experience in the simulator can be seen in the aircraft's trajectory and cyclic control inputs during the landing. Figure 29 shows the comparison of aircraft trajectories for the two MTS cases Benign and Optimised at two extreme WOD conditions, H00 45 kts SS5 and G45 35 kts SS5. The spatial deviation in the Benign MTS case (blue line) is larger and more erratic than the Optimised MTS case (red line), especially during the station-keeping MTE. This deviation in the Benign case is a result of the degraded motion cues which have led to the loss of task performance where the pilot commented: "*Poor motion cues making the task difficult*", and "*Difficult to perform the task accurately, especially in hover*". Whereas, in the Optimised case, enhanced motion cues were provided to the pilot resulting in better task performance capability where the pilot commented:

"*Stable performance in hover*", "*Improved task performance accuracy*" and "*Accurate performance in holding hover position*". These observations were further supported by analysing the pilot cyclic control stick activity.

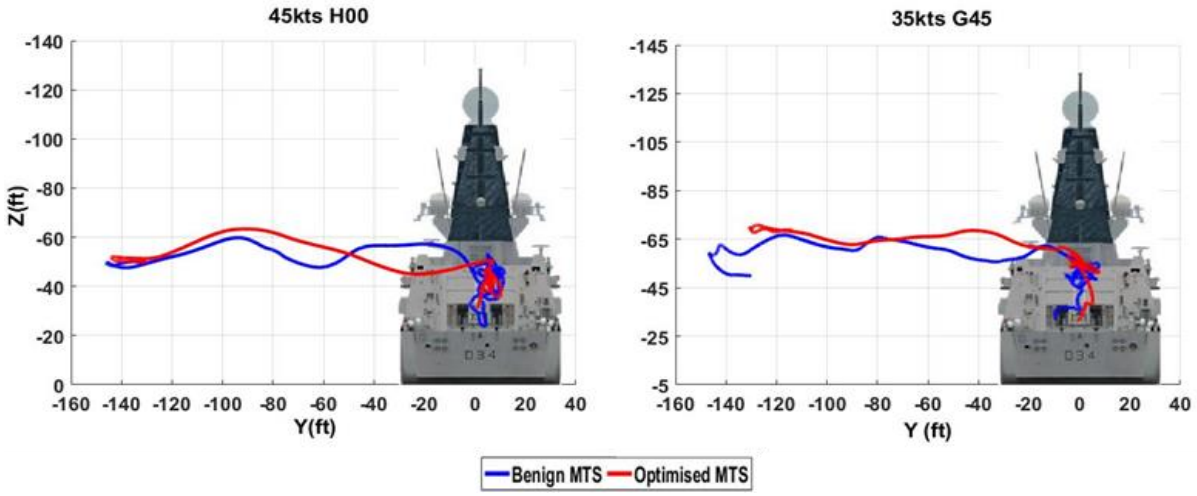

Fig. 29 Flight trial deck landing trajectory comparison for Benign and Optimised MTS, H00 and G45 WOD cases

Figure 30 shows the cyclic control inputs of the pilot for the two extreme cases, H00 45 kts and G45 35 kts, in the hover MTE only, where the pilot was asked to station-keep for 30 seconds. The central plot shows lateral (*XA*) vs longitudinal (*XB*) control activity while the outer plots show respective time histories. The pilot cyclic movement in the Benign MTS case while station-keeping is noticeably larger than in the Optimised MTS case at the same WOD condition. This is due to poor vestibular motion cues available to the pilot, which has hampered the overall simulation fidelity due to a larger mismatch between the visual and vestibular motion cues. This observation was supported by pilot comments where, in the Benign MTS case, the pilot commented: "*Control strategy reactive rather than interactive, need to see disturbance visually before reacting to it*" and "*Reactive strategy leads to higher control gains which subsequently leads to poor performance accuracy*". In contrast, in the Optimised MTS case, the pilot commented: "*Accurate controls and position keeping*". The results again demonstrate how the motion cues have influenced the control activity of the pilot, along with the landing performance.

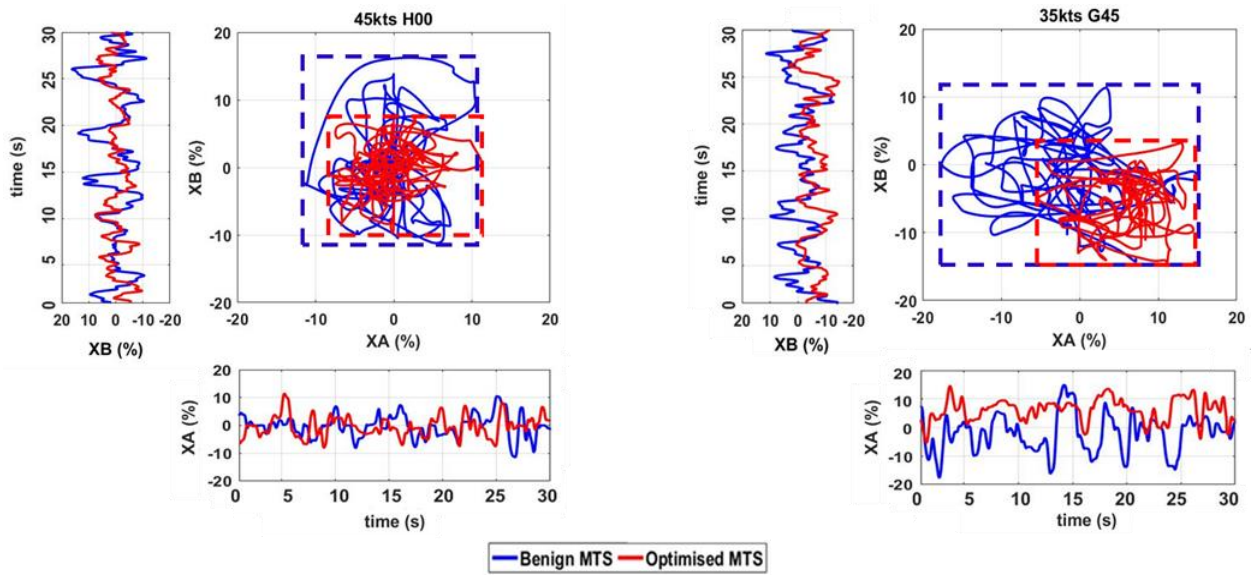

Fig. 30 Pilot cyclic control activity comparison in Hover MTE for Benign and Optimised MTSs, H00 and G45 WOD cases (trimmed reference)

To further analyse the effect of the motion cues, Figs. 31 and 32 show a frequency analysis comparing the simulator and simulated aircraft actual specific forces and angular rates obtained at the pilot's VC for the two extreme WOD cases tested, H00 45 kts and G45 35 kts, respectively. The results are shown for the actual specific force F_{sp}-x in x-axis and pitch rate ω_{sp}-y only. When using the Benign MTS, the simulator response is compromised resulting in loss of the peaks of the amplitude throughout the frequency range. While with the Optimised MTS the simulator reproduces the response of the simulated aircraft reasonably well, as predicted in the VMPE pre-trial optimisation phase in section IV.B, Figs. 21 and 22. This suggests that when using the Benign MTS, the simulator is not able to provide sufficient airwake turbulence feedback to the pilot via vestibular motion cues where the pilot has commented: "*Not able to physically feel airwake feedback disturbance from motion*", "*Motion not sufficient for perceiving airwake disturbances or ship motion*" and "*Can't physically feel anything, can only perceive visually*". Whereas, in the Optimised MTS, the pilot perceived more representative motion cues and airwake turbulence feedback due to better reproduction of the simulated aircraft accelerations by the simulator's motion platform. The pilot commented: "*Turbulence noticeable*", "*Airwake responses are more interactive*", "*Feeling gust response*" and "*More occurrence of airwake felt*". The results in Figs. 31 and 32 are therefore supported by the pilot comments and HMFR ratings along with the comparison of the pilot control activity detailed in the previous section for the same two extreme cases, H00 45 kts and G45 35 kts. Note the amplitude of FFT is normalized by the signal length to change the scale to the true amplitude.

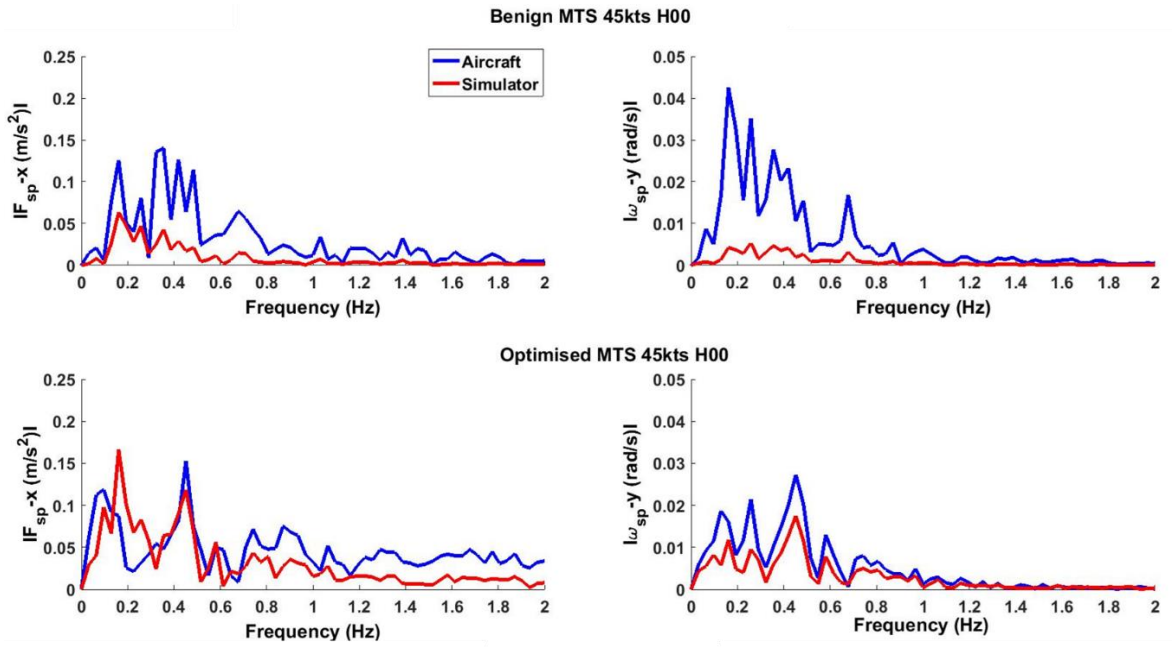

Fig. 31 Frequency Domain comparison of simulated aircraft and simulator actual specific forces and angular rates for Benign and Optimised MTS H00 45 kts case

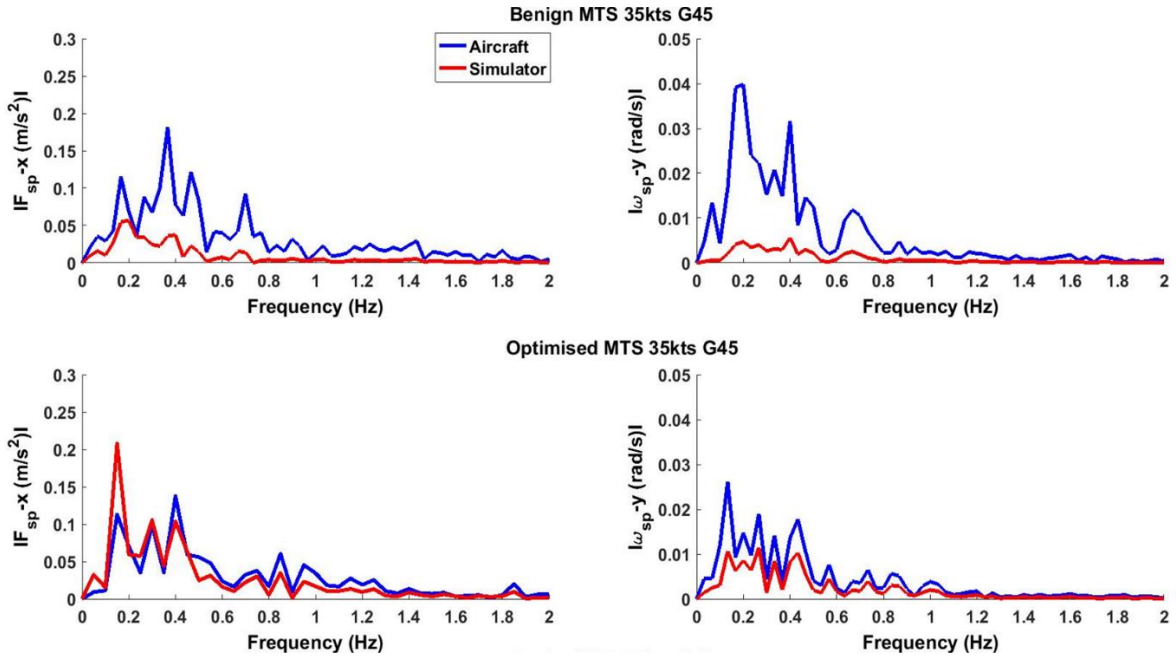

Fig. 32 Frequency Domain comparison of simulated aircraft and simulator actual specific forces and angular rates for Benign and Optimised MTS G45 35 kts WOD case

Finally, Fig. 33 compares the simulator and simulated aircraft angular rates during the hover MTE for the same extreme cases to see how the availability of the optimised vestibular motion cues has affected the aircraft dynamic

response. It can be seen that the helicopter roll (*P*) and pitch (*Q*) rates are large in the Benign MTS case, whereas the simulator response is extremely limited because only dominant motion cues are obtained from the visual scene which makes overall simulation system reactive as opposed to interactive. As the motion cueing is improved using the Optimised MTS, the helicopter angular rates for the same WOD case are relaxed while the simulator response is improved as well, making the overall simulation system interactive with improved task performance.

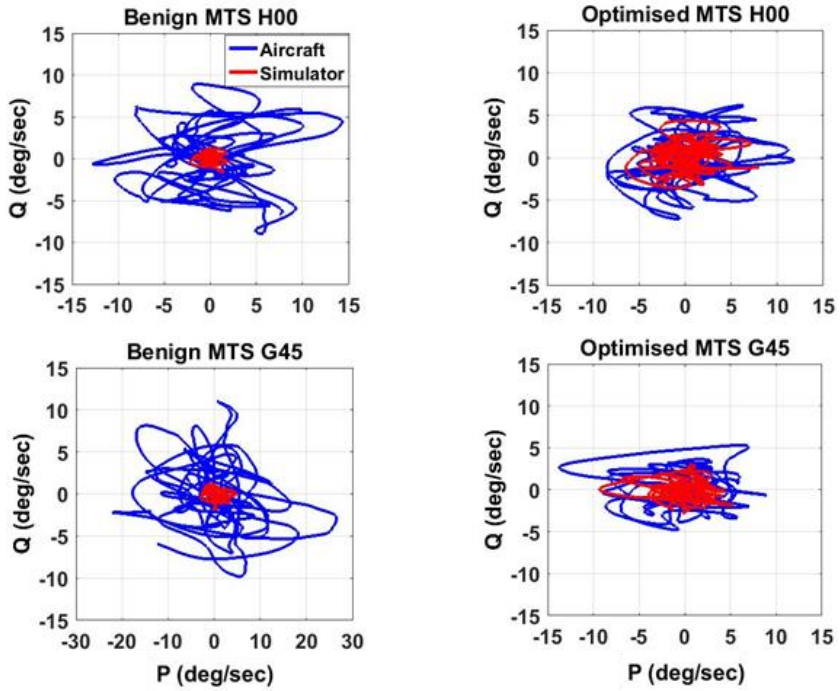

Fig. 33 Comparison of simulated aircraft and simulator angular rates for Benign and Optimised MTS, H00 and G45 WOD cases

VI.Conclusions

The flying environment above a ship's deck in strong winds and high seas is unique. The aircraft experiences significant unsteady forces and moments from the ship's turbulent airwake, which the pilot has to counteract while tracking a randomly moving landing spot. The research presented in this paper was aimed at establishing motion fidelity requirements for simulated HSDI operations to improve the overall fidelity of maritime rotorcraft simulators; this is key to their use in supporting future FOCFTs and deriving SHOLs. This improvement has been achieved using a new motion assessment and optimisation technique, VMPE. The paper has demonstrated the application of the VMPE technique in three phases: Pre-validation, Pre-trial optimisation and Flight trial experiment. Following are the key conclusions drawn from this work:

1. It was found that “high-fidelity” motion cueing becomes more desirable at higher airwake wind conditions than at lower winds, due to higher perturbations in the airflow over and around the ship’s landing deck and the subsequent disturbance of the helicopter. Pilot subjective HMFRs at lower WOD conditions (e.g., 15 and/or 25 kts) remained low and relatively constant when flying the simulator with any of the four motion tuning sets (Benign, Intermediate, Responsive or Optimised) where the visual motion cues were deemed to be solely sufficient for the pilot to accomplish the task. However, when the WOD airwake condition was increased to 35 kts and/or 45 kts the motion cueing for the pilot flying the simulator with the ‘Benign’ MTS degraded while it became more representative and operationally beneficial with the ‘Optimised’ motion set.
2. In the poorly tuned motion (i.e., Benign MTS), the dominant motion cues were obtained from the visual scene which makes the overall simulation system “reactive” as opposed to “interactive” resulting in poor position control. Whereas, using the Optimised MTS, the representative and synchronised motion cues helped the pilot to perform the task satisfactorily by minimising the mismatch between the vestibular and visual motion cues, hence producing better overall self-motion perception and position control.
3. In the quantitative comparison of the cyclic control activity of the pilot for the two extreme cases, Benign and Optimised MTS, it was found that the poorly tuned motion negatively influenced the control activity of the pilot. The control ranges were higher with the Benign MTS compared with the Optimised MTS, at the same WOD conditions. The reactive control strategy of the pilot leads to the higher control gains which subsequently leads to poor performance accuracy.
4. For the synchronised visual-vestibular motion perception of the pilot flying the HSDI task in the flight simulator, it is important for the simulator motion platform to effectively provide physical motion feedback of the external disturbances to the pilot. The frequency domain comparison of the actual specific forces and angular velocities at the pilot vestibular centre in the simulated aircraft and flight simulator was made for two extreme (maximum wind) conditions. It was found that with the Benign MTS the pilot only perceived the external disturbances of the airwake visually and not through physical motion, degrading the overall motion perception for the HSDI task. However, using the Optimised MTS the pilot felt more physical occurrence of the airwake in sync with the visual movement.
5. Angular rates of the simulated aircraft and flight simulator motion were compared to examine how the optimised vestibular motion cues affected the aircraft dynamic response in the simulator. It was indicated that the aircraft’s pitch and roll rate responses are relatively large in the Benign MTS case where the simulator response was very

limited. As the motion cueing was improved using the Optimised MTS, the helicopter angular rates were reduced while the simulator response was improved thus making the overall simulation system interactive. It is clear that the availability of appropriate vestibular motion cues affects the pilot's ability to perform the task.

6. Moreover, as well as the HSDI task examination, it was also important to capture the differences in the pilot workload during deck landings for the different MTSs. It was found that the motion cueing fidelity not only introduced differences in the control strategy, task performance and simulation fidelity perception but also the workload of the pilot. Providing poor motion cues to the test pilot impaired the prediction of the simulated SHOL boundary.
7. The VMPE technique has been shown to be useful for motion assessment and optimisation for a simulated shipboard landing task and provides a means of characterising vestibular motion perception in the aircraft and simulator. It can be used to derive task-specific motion tuning sets and for use in simulation trials prior to real-world testing.
8. From all the cases considered it was found that the Optimised MTS gave the lowest HMFR and workload ratings for all the WOD conditions tested; therefore, it can be regarded as a universal motion setting in a short stroke hexapod simulator for the lower as well as higher airwake conditions for simulated flight operations to a single spot ship.

Finally, it is recommended that the developed technique be employed on different simulators with larger motion envelopes, which will help further establish the motion fidelity requirements for simulated HSDI operations and determine if considerations need to be taken to improve VMPE predictions. The VMPE technique represents vestibular motion perception modality for the motion cueing optimisation, whereas self-motion perception, on the whole, uses other perceptual modalities, particularly the visual and proprioceptive/kinaesthetic sensory systems; these can be considered in a future version of the model. Additional test pilots will be invited to participate in further trials to assess the more challenging test points.

Acknowledgements

The authors would like to thank the industrial sponsors, QinetiQ and Dstl for funding the project under QinetiQ-Dstl Technology Fund. The authors would also like to thank: Dr Michael Jones from the DLR, Braunschweig, for providing access to the ADS-33 experimental data he obtained during the piloted simulation flight trial experiment

conducted at the UoL; Dr Sarah Scott ex-researcher at the UoL, for access to the ship airwakes and Andy Berryman, an ex-Royal Navy pilot, who conducted the simulation flight trials.

References

[1] Lumsden, B., and Padfield, G. D., "Challenges at the Helicopter-Ship Dynamic Interface," *24th European Rotorcraft Forum*, Marseilles, France, Sep. 1998.

[2] Fang, R., Krijns, H. W., and Finch, R. S., "Dutch/British Clearance Process," RTO AGARDograph 300: Helicopter/Ship Qualification Testing, Vol. 22, Flight Test Techniques Series, NATO Research and Technology Organization, 2003.

[3] Forrest, J. S., Owen, I., Padfield, G. D., and Hodge, S. J., "Ship-Helicopter Operating Limits Prediction Using Piloted Flight Simulation and Time-Accurate Airwakes," *Journal of Aircraft*, Vol. 49, No. 11, June 2012, pp. 1020-1031.
doi: 10.2514/1.C031525

[4] Forrest, J. S., Owen, I., Padfield, G. D., and Hodge, S. J., "Towards Fully Simulated Ship-Helicopter Operating Limits: The Importance of Ship Airwake Fidelity," *64th American Helicopter Society Annual Forum*, Montreal, April 2008.

[5] Advani, S., and Wilkinson, C., "Dynamic Interface Modelling and Simulation - A Unique Challenge," *Royal Aeronautical Society on Helicopter Flight Simulation*, London, Nov. 2001.

[6] Roscoe, M. F., and Wilkinson, C. H., "DIMSS - JSHIP's M&S Process for Ship helicopter Testing and Training," *AIAA Modeling and Simulation Technologies Conference and Exhibit*, California, USA, AIAA Paper 2002-4597, Aug. 2002.
doi: 10.2514/6.2002-4597

[7] Val, J., and Healey, V., "Simulating the Helicopter-Ship Interface as an Alternative to Current Methods of Determining the Safe Operating Envelopes," NAVAIR: Air Vehicle Division, 1986.

[8] Hoencamp, A., and Pavel, M. D., "Concept of a Predictive Tool for Ship–Helicopter Operational Limitations of Various In-Service Conditions," *Journal of the American Helicopter Society*, Vol. 57, No. 3, July 2012, pp. 1-9.
doi: 10.4050/JAHS.57.032008

[9] Hodge, S. J., Forrest, J. S., Padfield, G. D., and Owen, I., "Simulating the Environment at the Helicopter-Ship Dynamic Interface: Research, Development and Application," *The Aeronautical Journal*, Vol. 116, No. 1185, Nov. 2012, pp. 1155-1184.
doi: 10.1017/S0001924000007545

[10] Owen, I., White, M. D., Padfield, G. D., and Hodge, S., "A Virtual Engineering Approach to the Ship-Helicopter Dynamic Interface; A Decade of Modelling and Simulation Research at the University of Liverpool," *The Aeronautical Journal*, Vol. 49, No. 1246, Dec. 2017, pp. 1833-1857.
doi: 10.1017/aer.2017.102

[11] Wang, Y., White, M. D., Owen, I., Hodge, S., and Barakos, G., "Effects of Visual and Motion Cues in Flight Simulation of Ship-Borne Helicopter Operations," *CEAS Aeronautical Journal*, Vol. 4, No. 4, Dec. 2013, pp. 385-396. doi: 10.1007/s13272-013-0085-9

[12] Hodge, S. J., "Dynamic Interface Modelling and Simulation Fidelity Criteria," Ph.D. Dissertation, Flight Science & Technology Department, University of Liverpool, Liverpool, UK, 2010.

[13] Kelly, M. F., White, M. D., Owen, I., and Hodge, S. J., "Piloted Flight Simulation for Helicopter Operation to the Queen Elizabeth Class Aircraft Carriers," *43rd European Rotorcraft Forum*, Milan, Italy, Sep. 2017.

[14] Scott, P., Kelly, M. F., White, M. D., and Owen, I., "Using Piloted Simulation to Measure Pilot Workload of Landing a Helicopter on a Small Ship," *43rd European Rotorcraft Forum*, Milan, Italy, Sep. 2017.

[15] Watson, N., Kelly, M. F., Owen, I., White, M. D., and Hodge, S. J., "Computational and experimental modelling study of the unsteady airflow over the aircraft carrier HMS Queen Elizabeth," *Ocean Engineering*, Vol. 172, Dec. 2018, pp. 562-574. doi: 10.1016/j.oceaneng.2018.12.024

[16] Perfect, P., Timson, E., White, M. D., Padfield, G. D., Erdos, R., and Gubbels, A. W., "A Rating Scale for the Subjective Assessment of Simulation Fidelity," *The Aeronautical Journal*, Vol. 11, No. 1206, Aug. 2014, pp. 953–974. doi: 10.1017/S0001924000009635

[17] Perfect, P., White, M. D., Padfield, G. D., and Gubbels, A. W., "Rotorcraft Simulation Fidelity: New Methods for Quantification and Assessment," *The Aeronautical Journal*, Vol. 117, No. 1189, March 2013, pp. 235-282. doi: 10.1017/S0001924000007983

[18] EASA., "European Aviation Safety Agency Certification Specifications for Helicopter Flight Simulation Training Devices," 'CS-FSTD (H)', 2012.

[19] FAA., "Flight Simulation Training Device Initial and Continuing Qualification and Use," '14 CFR Part 60', 2016.

[20] Timson, E., Perfect, P., White, M. D., Padfield, G. D., Erdos, R., and Gubbels, A. W., "Subjective Fidelity Assessment of Rotorcraft Flight Training Simulators," *68th American Helicopter Society Annual Forum*, Fort Worth, TX, USA, May 2012.

[21] Pavel, M. D., White, M. D., Padfield, G. D., Roth, G., Hamers, M., and Taghizad, A., "Validation of Mathematical Models for Helicopter Flight Simulators Current and Future Challenges," *The Aeronautical Journal*, Vol. 117, No. 1190, April 2013, pp. 343–388. doi: 10.1017/S0001924000008058

[22] White, M. D., Perfect, P., Padfield, G. D., Gubbels, A. W., and Berryman, A. C., "Acceptance Testing and Commissioning of a Flight Simulator for Rotorcraft Simulation Fidelity Research," *Institution of Mechanical Engineers, Part G: Journal of Aerospace Engineering*, Vol. 227, No. 4, June 2012, pp. 663–686. doi: 10.1177/0954410012439816

[23] Manso, S., White, M. D., and Hodge, S., "An Investigation of Task-Specific Motion Cues for Rotorcraft Simulators," *AIAA Modeling and Simulation Technologies Conference*, San Diego, California, AIAA Paper 2016-2138, Jan. 2016.
doi: 10.2514/6.2016-2138

[24] Jones, M., White, M. D., Fell, T., and Barnett, M., "Analysis of Motion Parameter Variations for Rotorcraft Flight Simulators," *73rd American Helicopter Society Annual Forum*, Fort Worth, Texas, USA, May 2017.

[25] Hodge, S. J., Perfect, P., Padfield, G. D., and White, M. D., "Optimising the Roll-Sway Motion Cues Available from A Short Stroke Hexapod Motion Platform," *The Aeronautical Journal*, Vol. 119, No. 1211, Jan. 2015, pp. 23-44.
doi: 10.1017/S000192400001023X

[26] Hodge, S. J., Perfect, P., Padfield, G. D., and White, M. D., "Optimising the Yaw Motion Cues Available from a Short Stroke Hexapod Motion Platform," *The Aeronautical Journal*, Vol. 119, No. 1211, Jan. 2015, pp. 1-22
doi: 10.1017/S0001924000010228

[27] Jones, M., "Enhancing Motion Cueing Using an Optimisation Technique," *The Aeronautical Journal*, Vol. 122, No. 1249, March 2018, pp. 487-518.
doi: 10.1017/aer.2017.141

[28] Jones, M., "Motion Cueing Optimisation Applied to Rotorcraft Flight Simulation," *CEAS Aeronautical Journal*, Vol. 8, No. 3, Sep. 2017, pp. 523-539.
doi: 10.1007/s13272-017-0256-1

[29] Hodge, S., Perfect, P., Padfield, G. D., and White, M. D., "Optimising the Vestibular Cues Available from a Short Stroke Hexapod Motion Platform," *67th American Helicopter Society Annual Forum*, Virginia Beach, VA, May 2011.

[30] Reid, L. D., and Nahon, M. A., "Flight Simulation Motion-Base Drive Algorithms. Part 1: Developing and Testing the Equations," University of Toronto, Institute for Aerospace Studies Report. 296, 1985.

[31] Hosman, R. J. A. W., Cardullo, F. M., and Bos, J. E., "Visual-Vestibular Interaction in Motion Perception," *AIAA Modeling and Simulation Technologies Conference*, Oregon, AIAA Paper 2011-6425, Aug. 2011.
doi: 10.2514/6.2011-6425

[32] Nash, C. J., Cole, D. J., and Bigler, R. S., "A Review of Human Sensory Dynamics for Application to Models of Driver Steering," *Biological Cybernetics*, Vol. 110, Nos. 2-3, April 2016, pp. 91–116.
doi: 10.1007/s00422-016-0682-x

[33] Grundy, J. G., Nazar, S., Omalley, S., Mohrenshildt, M. V., and Shedden, J. M., "The Effectiveness of Simulator Motion in the Transfer of Performance on a Tracking Task is Influenced by Vision and Motion Disturbance Cues," *Human Factors*, Vol. 58, No. 4, June 2016, pp. 546–559.
doi: 10.1177/0018720816639776

[34] Grant, P. R., and Reid, L. D., "Motion Washout Filter Tuning: Rules and Requirements," *Journal of Aircraft*, Vol. 34, No. 2, March-April 1997, pp. 145-151.
doi: 10.2514/2.2158

[35] Nehaoua, L., Mohellebi, H., Amouri, A., Arioui, H., Espié, S., and Kheddar, A., "Design and Control of a Small-Clearance Driving Simulator," *IEEE Transactions on Vehicular Technology*, Vol. 57, No. 2, March 2008, pp. 736-746.
doi: 10.1109/TVT.2007.905336

[36] Du Val, R., and He, C., "Validation of the FLIGHTLAB Virtual Engineering Toolset," *The Aeronautical Journal*, Vol. 122, No. 1250, March 2018, pp. 519-555.
doi: 10.1017/aer.2018.12

[37] Gouverneur, B., Mulder, J. A., Van Paassen, M. M., Stroosma, O., and Field, E. J., "Optimisation of the SIMONA Research Simulator's Motion Filter Settings for Handling Qualities Experiments," *AIAA Modeling and Simulation Technologies Conference*, Austin, Texas, AIAA Paper 2003-5679, Aug. 2003.
doi: 10.2514/6.2003-5679

[38] Reid, L. D., and Nahon, M. A., "Response of Airline Pilots to Variations in Flight Simulator Motion Algorithms," *Journal of Aircraft*, Vol. 25, No. 7, July 1988, pp. 639-646.
doi: 10.2514/3.45635

[39] Casas, S., Coma, I., Portales, C., and Fernandez M., "Towards a Simulation-Based Tuning of Motion Cueing Algorithms," *Simulation Modelling Practice and Theory*, Vol. 67, Sep. 2016, pp. 137–154.
doi: 10.1016/j.simpat.2016.06.002

[40] Sinacori, J., "The Determination of Some Requirements for a Helicopter Flight Simulator Facility," Tech. Rep. CR-152066, NASA, 1977.

[41] Schroeder, J., "Helicopter Flight Simulation Motion Platform Requirements," NASA TP-1999- 208766, Ames Research Center, Moffet Field, California, US, July 1999.

[42] Asadi, H., Mohamed, S., Zadeh, D. R., and Nahavandi, S., "Optimisation of Nonlinear Motion Cueing Algorithm Based on Genetic Algorithm," *Vehicle System Dynamics*, Vol. 53, No. 4, Dec. 2015, pp. 526-545.
doi: 10.1080/00423114.2014.1003948

[43] Schroeder, J. A., Chung, W. W., and Hess, R. A., "Evaluation of a Motion Fidelity Criterion with Visual Scene Changes," *Journal of Aircraft*, Vol. 37, No. 4, July-Aug. 2000, pp. 580-587.
doi: 10.2514/2.2669

[44] Grant, P. R., and Reid, L. D., "PROTEST: An Expert System for Tuning Simulator Washout Filters," *Journal of Aircraft*, Vol. 34, No. 2, March-April 1997, pp. 152-159.

doi: 10.2514/2.2166

[45] Grant, P. R., Yam, B., Hosman, R., and Schroeder, J. A., "Effect of Simulator Motion on Pilot Behaviour and Perception," *Journal of Aircraft*, Vol. 43, No. 6, Nov.-Dec. 2006, pp. 1914-1924.
doi: 10.2514/1.21900

[46] Hosman, R., Advani, S., and Haeck, N., "Integrated Design of Flight Simulator Motion Cueing Systems," *The Aeronautical Journal*, Vol. 109, No. 1091, Jan. 2005, pp. 1-12.
doi: 10.1017/S000192400000049X

[47] Anon., "Manual of Criteria for the Qualification of Flight Simulation Training Devices," Vol. 1, Doc 9625, International Civil Aviation Organization, Third Edition, 2009.

[48] Hosman, R., and Advani, S., "Design and Evaluation of the Objective Motion Cueing Test and Criterion," *The Aeronautical Journal*, Vol. 120, No. 1227, May 2016, pp. 873-891.
doi: 10.1017/aer.2016.35

[49] Zaal, P. M. T., Schroeder, J. A., and Chung, W. W., "Transfer of Training on the Vertical Motion Simulator," *Journal of Aircraft*, Vol. 52, No. 6, Nov.–Dec. 2015, pp. 1971–1984.
doi: 10.2514/1.C033115

[50] Zaal, P. M. T., Schroeder, J. A., and Chung, W. W., "Objective Motion Cueing Criteria Investigation Based on Three Flight Tasks," *The Aeronautical Journal*, Vol. 121, No. 1236, Jan. 2017, pp. 163–190.
doi: 10.1017/aer.2016.119

[51] Zaal, P. M. T., Schroeder, J. A., and Chung, W. W., "Refinement of Objective Motion Cueing Criteria Based on Three Flight Tasks," *AIAA Modeling and Simulation Technologies Conference*, Grapevine, Texas, AIAA Paper 2017-1081, Jan. 2017.
doi: 10.2514/6.2017-1081

[52] Zaal, P. M. T., Schroeder, J. A., and Chung, W. W., "Objective Motion Cueing Criteria for Commercial Transport Simulators," *AIAA Modeling and Simulation Technologies Conference*, Atlanta, Georgia, AIAA Paper 2018-2935, June 2018.
doi: 10.2514/6.2018-2935

[53] Anon., "Aeronautical Design Standard Performance Specification Handling Qualities Requirements for Military Rotorcraft," ADS-33E-PRF, United States Army Aviation and Missile Command, Redstone Arsenal, AL, 2000.

[54] Carignan, S., Gubbels, A., and Ellis, K., "Assessment of Handling Qualities for the Shipborne Recovery Task - ADS 33 (Maritime)," *56th American Helicopter Society Annual Forum*, Virginia Beach, VA, May 2000.

[55] Asadi, H., Mohammadi, A., Mohamed, S., and Nahavandi, S., "Adaptive Translational Cueing Motion Algorithm Using Fuzzy Based Tilt Coordination," *Neural Information Processing*. Cham, Switzerland: Springer, Nov. 2014, pp. 474–482.
doi: 10.1007/978-3-319-12643-2_58

[56] Song, J. B., Jung, U. J., and Ko, H. D., "Washout Algorithm with Fuzzy-Based Tuning for a Motion Simulator," *KSME International Journal*, Vol. 17, No. 2, Feb. 2003, pp. 221–229.
doi: 10.1007/BF02984393

[57] Sivan, R., Ish-Shalom, J., and Huang, J. K., "An Optimal Control Approach to the Design of Moving Flight Simulators," *IEEE Transactions on Systems, Man, and Cybernetics*, Vol. 12, No. 6, Nov. 1982, pp. 818–827.
doi: 10.2514/6.2003-5676

[58] Reid, L. D., and Nahon, M. A., "Flight Simulation Motion-Base Drive Algorithms. Part 2, Selecting The System Parameters," University of Toronto, Institute for Aerospace Studies Report. 307, 1986.

[59] Telban, R. J., and Cardullo, F., "Motion Cueing Algorithm Development: Human-Centered Linear and Nonlinear Approaches," NASA technical report, NASA Langley Research Centre, Hampton, VA, USA, 2005.

[60] White, M. D., Dadswell, C., Fell, T., and Coates, R., "The Use of Modelling and Simulation to Give Students a HEADSTART into Aerospace Engineering," *AIAA Modeling and Simulation Technologies Conference*, SciTech Forum, Grapevine, Texas, USA, AIAA Paper 2017-1763, Jan. 2017.
doi: 10.2514/6.2017-1763

[61] Jones, M., "Enhancing Motion Cueing Using an Optimisation Technique," *Proceedings of the Rotorcraft Virtual Engineering Conference*, Royal Aeronautical Society, Liverpool, UK, Nov. 2016.

[62] Heerspink, H. M., Berkouwer, W. R., Stroosma, O., Paassen, M. M., Mulder, M., and Mulder, J. A., "Evaluation of Vestibular Thresholds for Motion Detection in the SIMONA Research Simulator," *AIAA Modeling and Simulation Technologies Conference and Exhibit*, San Francisco, California, AIAA Paper 2005-6502, Aug. 2005.
doi: 10.2514/6.2005-6502

[63] Groen, E. L., Wentink, M., Valente Pias, A. R., Mulder, M., and Van Paassen, M. M., "Motion Perception Thresholds in Flight Simulation," *AIAA Modeling and Simulation Technologies Conference and Exhibit*, Keystone, Colorado, AIAA Paper 2006-6254, Aug. 2006.
doi: 10.2514/6.2006-6254

[64] Memon, W. A., White, M. D., Owen, I., and Robinson, S., "Preliminary Progress in Establishing Motion Fidelity Requirements for Maritime Rotorcraft Flight Simulators," *74th Annual Forum & Technology Display Forum*, Phoenix, Arizona, USA, May 2018.

[65] McTaggart, K., "Validation of ShipMo3D Version 1.0 User Applications for Simulation of Ship Motion," Technical Memorandum, DRDC Atlantic TM 2007-173, Aug. 2007.

[66] Roscoe, A. H., and Ellis, G. A., "A Subjective Ratings Scale for Assessing Pilot Workload in Flight: A Decade of Practical Use," RAE Technical Report, RAE-TR-90019, 1990.

Appendix

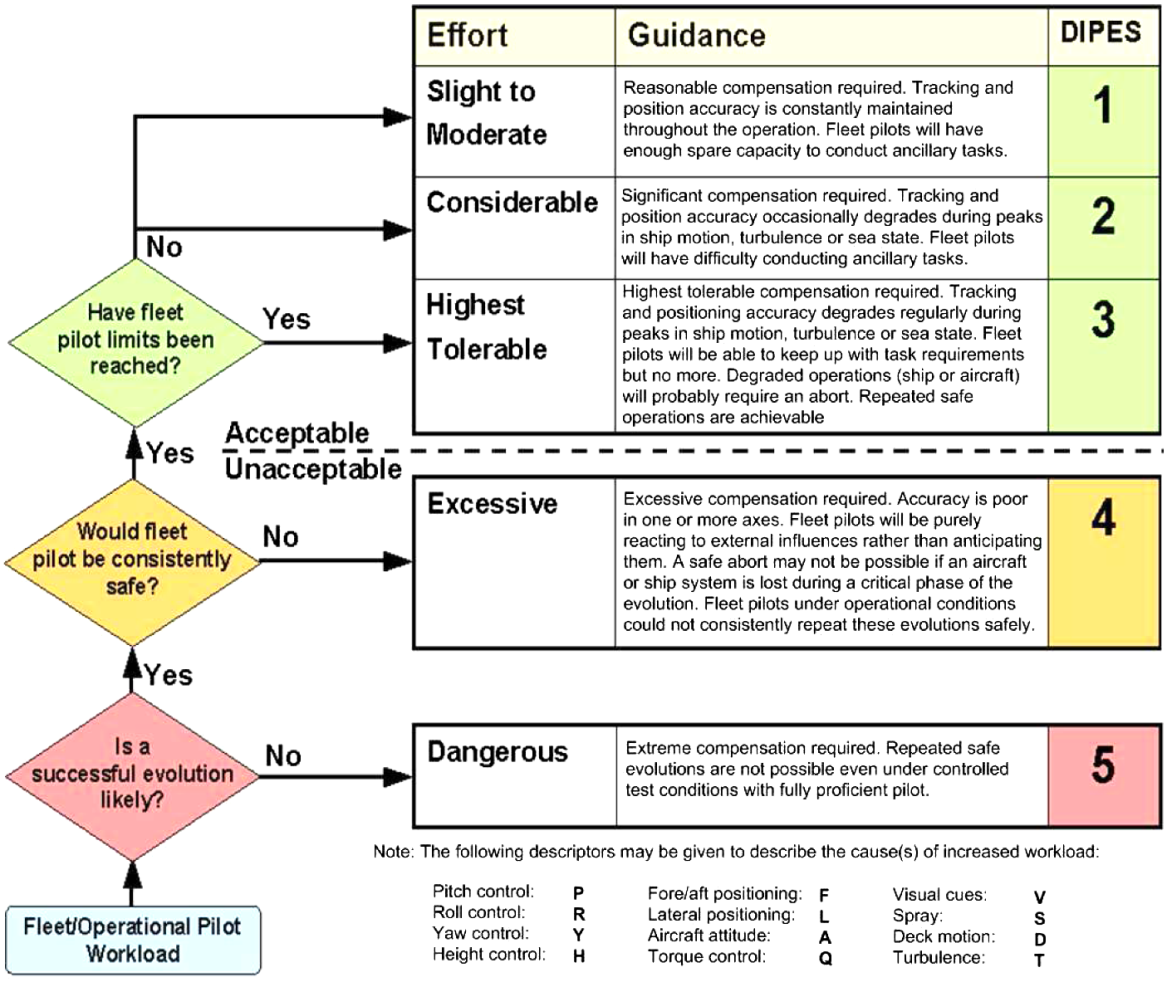

Fig. 34 Deck Interface Pilot Effort Scale (DIPES) rating scale [2]

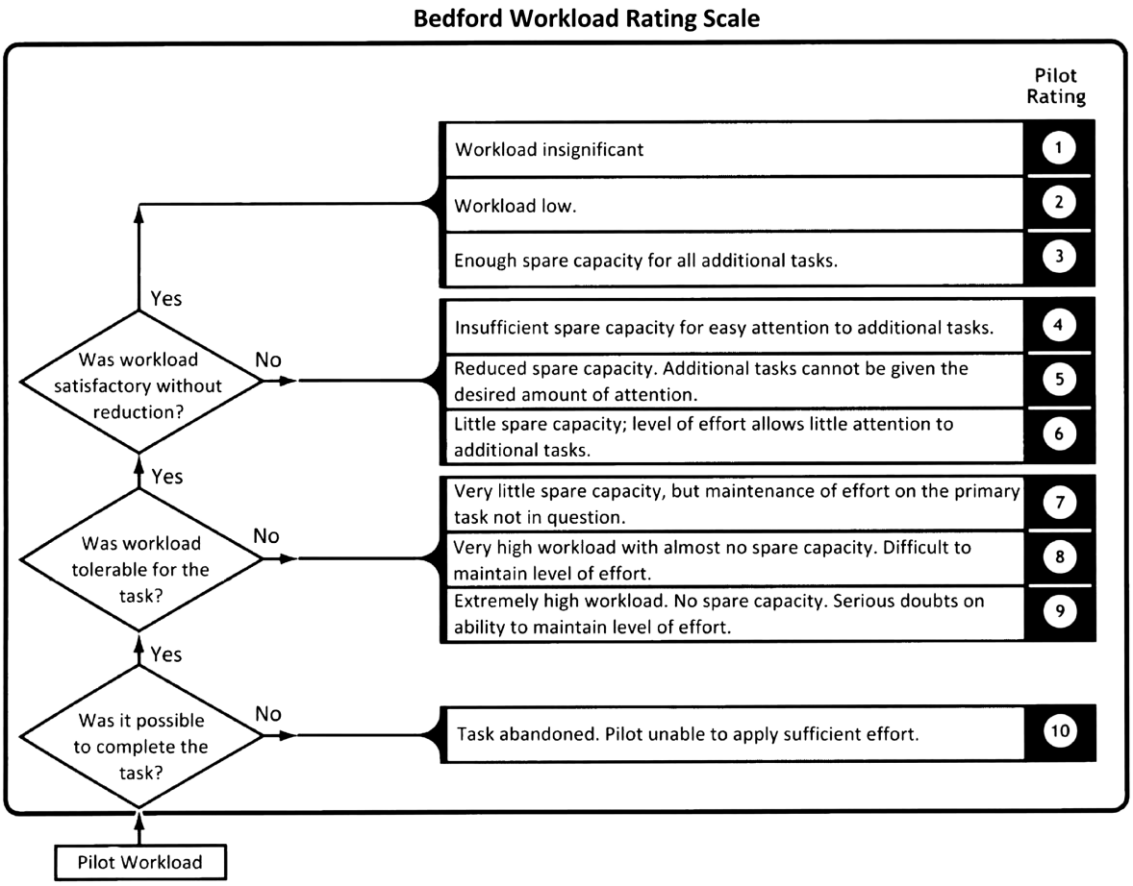

Fig. 35 Bedford Workload Rating (BWR) scale [66]